

ISSN 0972-0480 • Vol. 25 No. 9 • September 2022

IIM METAL NEWS

A monthly publication of The Indian Institute of Metals



ADVANCED MATERIALS



Accelerating towards a #GreenerStrongerSmarter future

Hindalco is proud to be recognised as the World's Most Sustainable Aluminium Company* again this year



*Dow Jones Sustainable Indices 2020 & 2021

IIM METAL NEWS

Vol. 25 No. 9 September 2022

Chief Editor

Dr. N Eswara Prasad

Printed and Published by
Shri Kushal Saha, Secretary General IIM,
on behalf of “The Indian Institute of Metals”,
and
printed at Print Max, 44, Biplabi Pulindas Street,
Kolkata-700009 and
published at ‘Metal House’, Plot 13/4, Block
AQ, Sector V, Salt Lake, Kolkata-700091, West
Bengal, India

E-mail: secretarygeneral.iim@gmail.com,

iimmetalnews@yahoo.com

Phone: 033-2367 9768 / 2367 5004

Website: www.iim-india.net

Fax: (033) 2367 5335

Facebook -

<https://www.facebook.com/TheIndianInstituteofMetals/>

Instagram -

<https://www.instagram.com/indianinstituteofmetals/>

LinkedIn -

<https://www.linkedin.com/company/the-indian-institute-of-metals/>

Twitter -

https://twitter.com/iimetals_india

The IIM Metal News and The Indian Institute of Metals do not accept any responsibility for the statements made and the opinion expressed by the author(s) in the technical articles

Interview of Prof. B. S. Murty

5

Exclusive in IIM MN: The Director of IIT Hyderabad talked about the importance of having collaboration between industry and academia

Special Feature

7

Brief about IIT Hyderabad (IITH)

Technical Article

9

Sensitisation Study on View Factor Update in Investment Casting Simulation

Saurabh Kumar, Daisy Priya Tigga and Dibyendu Chatterjee

News Updates

31

Chapter Activities

31



THE INDIAN INSTITUTE OF METALS

PATRONS

Mr R M Dastur

Dr Baba Kalyani

ADVISORY COMMITTEE OF FORMER PRESIDENTS

Mr M Narayana Rao
Mr H M Nerurkar
Prof K Chattopadhyay

Dr R N Patra
Mr S S Mohanty
Prof Indranil Manna
Dr Samir V Kamat, Convenor

Dr Biswajit Basu
Mr Anand Sen
Dr U Kamachi Mudali

COUNCIL FOR THE YEAR 2022-23

PRESIDENT

Dr Samir V Kamat

VICE PRESIDENT & CHAIRMAN

Non- Ferrous Division

Mr Satish Pai

VICE PRESIDENT & CHAIRMAN

Ferrous Division

Mr Sajjan Jindal

VICE PRESIDENT & CHAIRMAN

Metal Science Division

Prof B S Murty

IMMEDIATE FORMER PRESIDENT

Mr T V Narendran

SECRETARY GENERAL

Mr Kushal Saha

HON TREASURER

Mr Somnath Guha

CONTROLLER OF EXAMINATIONS

Prof P K Mitra

CHIEF EDITOR, TRANSACTIONS

Dr S V S Narayana Murty

CHIEF EDITOR, IIM METAL NEWS

Dr N Eswara Prasad

Jt. SECRETARY

(Office of President)

Dr R Balamuralikrishnan

MEMBERS

Mr Arun Kumar Agrawal
Dr Murugaiyan Amirthalingam
Prof Amit Arora
Dr Nagamani Jaya Balila
Dr Suddhasatwa Basu
Dr Amit Bhattacharjee
Dr Debashish Bhattacharjee
Mr Atanu Bhowmick
Mr P Chakraborty
Dr Indranil Chattoraj
Dr Vikas Chaudhari
Dr D DeSarkar
Prof Manojit Ghosh
Mr Prabhaskar Gokarn
Mr Praveen Jain
Dr S K Jha
Dr Vikas Jindal

Dr J Krishnamoorthi
Mr Anjani Kumar
Dr Mukesh Kumar
Dr Atish Mandal
Prof B K Mishra
Mr Bibhu Prasad Mishra
Dr Suman Kumari Mishra
Prof Sushil K Mishra
Mr Arun Misra
Prof Rahul Mitra
Dr D P Mondal
Ms Soma Mondal
Mr K Nagarajan
Mr Dilip Oommen
Mr Ambika Prasad Panda
Mr Gajraj Singh Rathore
Dr Asim K Ray

Dr G Madhusudhan Reddy
Mr Barun Roy
Mr Bhaskar Roy
Mr Sanjay Sharma
Mr Vidya Ratan Sharma
Mr Arun Kumar Shukla
Mr A K Singh
Prof Amarendra Kumar Singh
Dr Bimal P Singh
Mr Brijendra Pratap Singh
Mr Deependra Singh
Mr Lokendra Raj Singh
Prof Sudhansu Sekhar Singh
Dr Dheepa Srinivasan
Prof Satyam Suwas
Dr Vilas Tathavadkar
Dr B Venkatraman

FORMER PRESIDENTS

1946-48	Late J J Ghandy	1977-78	Late V A Altekhar	1992-93	Late A C Wadhawan	2007-08	Late Srikumar Banerjee
1948-50	Late P Ginwala	1978-79	Late T R Anantharaman	1993-94	Late R Krishnan	2008-09	Mr L Pugazhenthay
1950-52	Late Phiroz Kutar	1979-80	Late P L Agrawal	1994-95	Dr S K Gupta	2009-10	Dr Sanak Mishra
1952-54	Late G C Mitter	1980-81	Late EG Ramchandran	1995-96	Mr R N Parbat	2010-11	Dr D Banerjee
1954-56	Late M S Thacker	1981-82	Late C V Sundaram	1996-97	Late P Rodriguez	2011-12	Mr M Narayana Rao
1956-58	Late K S Krishnan	1982-83	Late Samarungavan	1997-98	Late S Das Gupta	2012-13	Mr H M Nerurkar
1958-60	Late S K Nanavati	1983-84	Late J Marwaha	1998-99	Dr C G K Nair	2013-14	Prof K Chattopadhyay
1960-62	Late G K Ogale	1984-85	Late A K Seal	1999-00	Prof S Ranganathan	2014-15	Dr R N Patra
1962-65	Late Dara P Antia	1985-86	Dr J J Irani	2000-01	Mr V Gujral	2015-16	Mr S S Mohanty
1965-67	Late B R Nijhawan	1986-87	Late Y M Mehta	2001-02	Late P Parvathisem	2016-17	Prof Indranil Manna
1967-70	Late M N Dastur	1987-88	Dr V S Arunachalam	2002-03	Late P Ramachandra Rao	2017-18	Dr Biswajit Basu
1970-72	Late Brahm Prakash	1988-89	Late S R Jain	2003-04	Late S K Bhattacharyya	2018-19	Mr Anand Sen
1972-74	Late P Anant	1989-90	Late L R Vaidyanath	2004-05	Dr T K Mukherjee	2019-20	Dr U Kamachi Mudali
1974-76	Late FAA Jasdanwalla	1990-91	Dr P Rama Rao	2005-06	Late Baldev Raj	2020-21	Prof Amol A Gokhale
1976-77	Late S Visvanathan	1991-92	Dr T Mukherjee	2006-07	Mr B Muthuraman	2021-22	Mr T V Narendran

FORMER SECRETARIES / SECRETARY GENERALS*

1946-57	Late Dara P Antia	1968-76	Dr M N Parthasarathi	1986-97	Late S S Das Gupta	2006-13	*Mr J C Marwah
1958-67	Mr R D Lalkaka	1977-86	Late L R Vaidyanath	1997-06	Mr J C Marwah	2013-15	*Mr Bhaskar Roy
						2015-18	*Mr Sadhan Kumar Roy

Interview

Director of Indian Institute of Technology Hyderabad Prof. B. S. Murty



Prof. B. S. Murty
 Director, IIT Hyderabad

1) The IIT system in India has established itself as globally renowned education institutes. During this long journey of our IITs, how has it viewed the importance of industrial collaboration?

From the inception, the bright faculty and student fraternity of all the IITs contributed to industrial collaborations through valuable consultancies. However, the number of sponsored projects from industry used to be less earlier. In the past 5-10 years, the number of industry sponsored projects has increased along with consultancy projects. Industries are also coming forward to set up Centres of Excellence at IITs, which have fostered industrial collaborations.

2) How should academia set the focus towards research relevant for industrial applications?

Academia first should create an environment in their institutes that foster stronger relationships with industry. Let me share the experiments that we have done at IITH.

- a) We have revised our BTech curriculum to incorporate a semester-long internship with 6 credits in the 6th semester.
- b) We have introduced a mandatory 1-credit course on Industry lectures for the MTech students, wherein 12-14 industries are invited to share the exciting developments in their industry.
- c) We ask the industry to provide problem statements for MTech students to take them as their MTech projects. I can confidently say that 30-40 % of our MTech projects are industry defined problems. We are striving to increase this to 60-70%.
- d) We encourage industry professionals to pursue their PhD at IITH, we have waived the residential requirement.
- e) We have also started 10 flexible online MTech programs for working professionals.
- f) We have started a number of industry-oriented and interdisciplinary MTech (Energy, Sensors, Additive manufacturing, E-waste management, Smart mobility, Medical device innovation, Ophthalmic Engineering) and BTech programs (Computational Engineering).

All these measures are helping IITH develop stronger relations with industry, which would encourage industry relevant research at IITH.

3) Please tell us a few success stories where research incubated in academia translated into successful industrial products.

While there are many success stories, I will talk about 3 of them:-

- a) Pure EV has been incubated at IITH, mentored by Dr. Nishanth from MAE dept, which is now producing about 2000 E-two wheelers a
- b) Wisig is a telecom-based start-up mentored by Prof. Kiran of EE dept, that is creating ripples in the field of 5G and 6G and has produced the first 5G enabled NB-IOT Chip from India.

c) Aerobiosys has been mentored by Prof. Renu of BME dept. and is producing the world's best ventilator at an affordable price.

4) Do you think major industries should also establish research cells in academia to forge a stronger research partnership?

Yes, Surely. A number of such Cells/ CoEs/ Schools are being set up at IITH; Centre for Healthcare Entrepreneurship, NVidia Centre, CoE on AI, ITIC, Suzuki Innovation Centre, FABCI, School of Innovation, School of Sustainability are some examples.

5) Can you please highlight a few successful start-ups incubated in academia?

For IITH, the answer to 3) above gives an idea of a few successful start-ups.

6) Do you think that a strong industry-academia partnership is the key factor for the advancement in engineering/ science in the western world? If so, then why could such an ecosystem not be nucleated in our country?

Yes, as I said, this is needed in India as much as elsewhere in the world. The advanced countries have this Academic-Industry research focus not only established in most areas, they also institutionalised and regularised this as a standard practice and immensely benefited. Many HE institutes in India have started similar engagements with industry and some of them being implemented at IITH have been highlighted in this note.

7) According to you, what are key policy and administrative reforms that should take place to enhance inter-dependency between industry and academia?

Each department in an engineering institute should be mentored by a few industries, where the students should do long term internships. The faculty should be encouraged to spend their summers in the industry not only to widen their knowledge-base but also to initiate collaborative research. Similarly, industry-professionals should take part in curriculum-design and also teach as Professors of Practice, a few practice-based courses. IITH has created TRP (Technology Research Park) with 1.5 Lakh sq.ft area for industries to take space on the campus and work together with faculty for a synergistic growth. In order to create an innovation culture at IITH, we have started providing BUILD (Bold and Unique Ideas Leading to Development) projects to students by calling for Innovative proposals from students twice a year. The chosen ideas are provided with Rs. 1 lakh financial support to begin with and even a semester-break with 6 credits, if needed. Technology Innovation Park (TIP) with 1.5 lakh sq.ft area has been created at IITH for providing space for start-ups. The philosophy of IITH is reflected in its motto that defines IITH as "Inventing & Innovating in Technology for Humanity".

8) How do you think, academia can play an important role in infusing innovation in Indian Industries, so that we can stride ahead towards 'Atmanirbhar Bharat' and subsequently to Global Leadership?

Efforts should be made to expose both the faculty and industry professionals to each other's environment. IITH has started an MTech program on Medical Device Innovation, jointly with AIG Hyderabad, where the student spends 4 months in a hospital (immersion) and identifies a problem at the end and works on it to create a prototype at the end of the 2-year program. We also started, jointly with CMET, an MTech on E-waste management, where the students do their projects in CMET and other industries. We also started an MTech in Ophthalmic Engineering together with LVPEI. We now have an MSc program on Medical Physics with Basavatarakam Oncology Institute, and the students of this program spend one year in the hospital and come out as Radiation experts.

We established a DRDO Cell at IITH, which has been working on the research problems of DRDO. This Cell is now converted into DIA (Defence-Industry-Academia) CoE. We have also started taking about 10 PhD students every year, who would work on research problems defined by DRDO. This year, we started a BTech program in IC Design & Technology, an MTech program in Systems Packaging and another MTech in Semiconductor Materials and Devices, to support the Indian Semiconductor Mission. Our BTech Curriculum is adopted by AICTE to start similar BTech program in colleges affiliated to AICTE. All these efforts would strengthen the technology base in India and create future-ready and competent human resources that would not only make India *Atma Nirbhar* but also a Global leader.

Special Feature Brief about IIT Hyderabad (IITH)

Indian Institute of Technology Hyderabad (IITH) is one of the second generation IITs established in 2008. IITH has been consistently ranked in the top 10 institutes in India for Engineering in both NIRF and QS rankings, thanks to the excellent work by its 290+ faculty, 270+ staff and 4200+ students. Among the students, 1200 are PhD students and 1300 are PG students, clearly indicating the research focus of IITH. Some of the unique contributions of IITH are in health care innovation, 5G/6G, autonomous navigation, additive manufacturing.

created 1000+ jobs and Rs. 800+ Cr Revenue. IITH has created Technology Innovation Park of 1.5 lakh sft space for supporting startups. IITH has Established incubators like Centre for Healthcare Entrepreneurship (CfHE) for medical innovations and FabCI for unique fabless chip design.



Iconic Tower

IITH has 18 departments, some of them being unique such as Department of AI, Design, Liberal Arts, Climate Change, Entrepreneurship & Management, Heritage Science & Technology. IITH has been striving in innovation domain, which has led to its being ranked 7 in ARIIA Innovation ranking of Govt. of India, which is better than two of the first generation IITs such as KGP and Guwahati. IITH defines its motto as “Inventing and Innovating in Technology for Humanity (IITH)”. In the last 5 years it has mentored 100+ startups, which have



Academic Block

IITH believes that education should be student centric and has brought out an innovative curriculum to provide more flexibility in learning through fractal academics, semester-long internship, more free electives, double major, several liberal/creative arts courses. It has brought out an innovation policy which encourages students to work on innovations taking a semester break if needed with 6 credits.



Departmental Building

IITH strongly believes that engineering education should be industry oriented. It has brought out several unique BTech programs in AI, Biomedical Engineering, Bioinformatics, Industrial Chemistry,

IC Design & Technology and Computational Engineering (possibly the first Interdisciplinary BTech program of India). Several other industry-oriented measures such as a mandatory 1-credit course on “Industry Lectures”, a large fraction of MTech projects being on industry defined problems. Several new industry-oriented MTech programs such as Additive manufacturing (with DRDO support), E-waste resource engineering & management (jointly with C-MET, Hyderabad, and with MeitY support), Medical device innovation (jointly with AIG, Hyderabad), Energy science & technology, Integrated sensor systems, Network & information security, Polymers & biosystems engineering and Smart mobility, systems packaging, Semiconductor materials & Devices, Ophthalmic Engineering (jointly with LVPEI), Techno-entrepreneurship and an MSC in Medical Physics (with Basavarakam Hospital). IITH has also started about 10 online MTech programs to reach out to working professionals. In another move to support industry and R&D lab personnel, IITH waived the need of semester-long residential requirement for PhD.

To contribute towards Atmanirbhar Bharat, a DRDO Centre of Excellence (DIA CoE) has been established at IITH. Technology Innovation Hub on Autonomous Navigation (TiHAN) under DST NMICPS has been established with first of its kind Testbed for autonomous vehicles in an Indian academic institute.

A Centre of Excellence for Medical devices has been set up with the funds from ICMR. Another Centre of Excellence for Transportation Research has been set up with the funds from NHAI. A school of Innovation & Entrepreneurship is being established with the support of Shibodhi Foundation and Cyient Foundation. The school is planning to start a BTech program on Techno-entrepreneurship. A school of Climate Change & Sustainability is being established with the support of Greenko. The school is planning to state BTech and MTech programs on Sustainability soon. A Research Centre for Eye Care is being established with the support of LV Prasad Eye Institute. Technology Research Park (TRP) with 150,000 sft space has been established for improving collaborations with industry.



IITH Hostel

Special Editor & Chief Reviewer : Dr. Shantanu Chakrabarti

EDITORS

Dr Monojit Dutta
Dr R Raghavendra Bhat
Prof J Dutta Majumdar
Prof Sudhanshu Shekhar Singh
Dr Mithun Palit

CORRESPONDENTS

Dr Chiradeep Ghosh (Jamshedpur)
Sri Rishabh Shukla (Pune)
Dr Ramen Datta (Delhi)
Dr L Ramakrishna (Hyderabad)
Sri Lalan Kumar (Visakhapatnam)
Sri A S Parihar (Kanpur)

Technical Article

Sensitisation Study on View Factor Update in Investment Casting Simulation

Saurabh Kumar¹, Daisy Priya Tigga and Dibyendu Chatterjee

Modern turbine-components are manufactured via investment casting process and are cast in vacuum induction and melting furnaces using nickel-based superalloys. The casting process parameters namely, temperature of the shell mould, pouring temperature and withdrawal rate, play a critical role in the quality of the final component; especially during production of directionally solidified castings. The optimisation of casting parameters by experimentation is a time and resource consuming process. Therefore, advanced simulation techniques are now being used to develop these casting procedures. FEM-based simulation has enabled us to estimate detailed thermal history of these casting processes and to understand the solidification characteristics. These simulation procedures are limited by computational hardware resources and also the time taken for computation. We have therefore focused in the present study on 'View factor update interval'(VFUI), a simulation parameter which determines the frequency of heat exchange calculations during the simulation process. The effect of VFUI at 1, 2, 5 & 10 mm withdrawal of mould on the computation time and accuracy is studied by noting its effect on thermal profile, mushy zone and solidification parameters in a directional solidification process of CM247 LC. Based on the study, the optimum VFUI for carrying out a simulation of directional solidification has been proposed.

Key words : Directional solidification, Radiation, View factor, VFUI, Thermal evolution, Thermal profile.

1. Introduction

1.1. General

Nickel-based superalloys have emerged as the most favourable choice of material for the manufacture of hot end components in advanced gas turbine engines. These alloys retain their mechanical properties at elevated temperatures and possess good oxidation/corrosion resistance [1-4]. In order to keep pace with the increasing turbine entry temperature (TET), the high temperature capability of these alloys have been enhanced over the years by improving their compositions and processing methods. The high temperature capability has been enhanced by introducing increasing quantities of

refractory elements such as W, Re and Ta [5]. Further improvements have also been achieved by adopting components with complex internal cooling channels.

Apart from the development in alloy systems, the microstructure has also been modified over the years. The processing routes were altered to produce more robust and suitable microstructure in the components. Equiaxed microstructure was modified to columnar grained microstructure by allowing directional solidification of the casting. Absence of grain boundaries in the transverse loading direction increased the working life of the components. Further improvement in the processing techniques for directional solidification led to the viability of producing single crystal components. Single crystal castings favoured excellent creep resistance and significantly increased the working life of these components [6, 7].

Modern gas turbine engine parts such as blades and nozzle guide-vanes of the nozzle have become so complex and strong as their fabrication is possible only through investment casting technique. Investment casting method for a superalloy component involves its casting in a ceramic shell mould. This process is carried out in a vacuum induction melting & casting furnace. Prior to pouring the liquid metal into the shell mould, it is typically heated to a high temperature (up to 1500 °C).

In case of equiaxed casting, the molten metal is poured into the mould inside the vacuum melting furnace and allowed to cool. In directional solidification casting process, the shell mould is placed over a water cooled copper chill plate which acts as the first sink for heat extraction and start the process of solidification. This is schematically shown in Fig.1.1. After the liquid metal is poured into the mould, it is withdrawn from the hot zone at a controlled rate, while heat extraction continues by radiation. In this process, the metal pouring temperatures, the temperature of the mould and the withdrawal rate play important roles in determining the final microstructure of the casting [8, 9].

Determination of the right casting parameters is crucial to produce sound castings. Experimental optimization

¹Author for correspondence: Saurabh Kumar, DMRL, Kanchanbagh, Hyderabad – 500058. Phone: 04024586314. Email: sanskarta@gmail.com. Fax: 040-24343006.

of these parameters is a long drawn and expensive process involving wastage of casting materials. Therefore, computational techniques using FEM analysis are employed to reduce the number of trials. The advancements in hardware technology and simulation tools have made it possible to predict the various aspects of casting process such as heat transfer and solidification with a fair degree of accuracy.

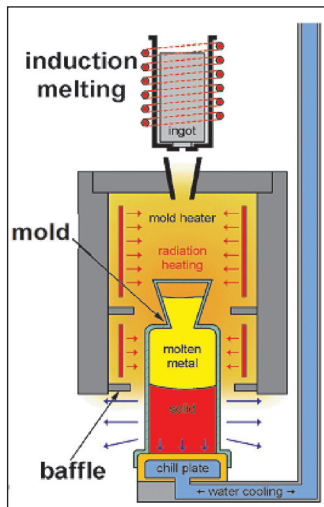


Fig.1.1 : Schematic of DS Process

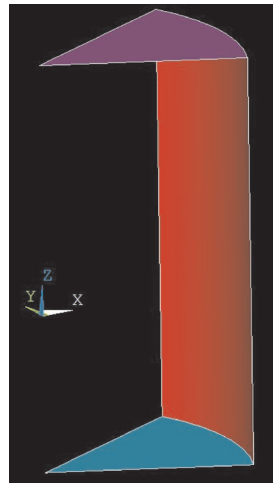


Fig.2.1 : Enclosure used in the simulation

1.2. Objective

The pouring of molten metal into the ceramic shell mould is followed by the withdrawal of the shell mould from the hot zone to the cold zone of a directional solidification (DS) furnace. The primary mode of heat transfer is initially conduction followed by radiation with the progress of withdrawal [2, 10]. Heat from the shell mould is radiated in all possible directions. With the progress of withdrawal, the heat transfer between the two particular surfaces involved keeps changing.

This exchange of energy between any two surfaces is defined by the 'view factor' or its synonyms 'shape factor', 'F factor', or 'configuration factor'. The view factor can be defined as the fraction of energy which is intercepted by a surface from a radiating surface [11]. This interception is governed by the way the surfaces and elements involved in radiation see each other. With the progress of shell withdrawal from hot zone to cold zone, the surfaces are exposed to new radiation conditions, new surfaces are exposed to each other and at the same time the angles and distances between the different surfaces and elements involved in radiation also keep changing. Therefore, while simulating the casting process, the view factor must be calculated for each of the pair of new surfaces exposed and for the changed position of radiating elements at regular intervals of time.

This calculation is both resource and time-consuming

and hence important to have the optimum intervals for updating the view factor in the simulation. If the view factors are calculated very frequently, the time taken for arriving at a solution becomes too long; on the contrary, if the frequency is too low, then the accuracy in computation is lost. Therefore, there needs to be an optimum interval for calculating the view factor.

The present study is aimed at examining the sensitivity of results with respect to the frequency of updating the view factor. Simulation has been carried out for investment casting of cylindrical superalloy (CM247 LC) rods using various view factor update frequencies and their effects on thermal evolution, thermal profile, thermal gradient and cooling & solidification rates have been studied.

2. Simulation Methodology

2.1. The physics

Solidification in investment casting is a result of heat dissipation by initially dominant heat conduction and subsequently radiation which becomes dominant soon after the mould begins to be withdrawn. The convection mode of heat transfer is irrelevant as the process is carried out in a vacuum furnace. The gradients imposed in solid phase and liquid phase determine the movement of solid-liquid front [12-14]. The process physics has been discussed here in two parts, namely solidification and radiation. The physics of solidification has been briefly described since it has already been discussed in our previous reports [15]. The physics of radiation however has been discussed in detail.

2.1.1. Solidification

The process of computational solidification is defined by the Stefan Problem [16]. This is a mathematical formulation widely used in engineering problems. The Stefan problem is probably the simplest mathematical model for a phenomenon involving change of phase. In our case, it is a set of mathematical equations which defines the movement of solid-liquid interface. These mathematical equations are governed by the heat flow across the solid-liquid interface [17, 18]. This solid-liquid interface, also called as a 'boundary' is non-stationary in a solidification process and hence this problem is considered as an example of 'free or moving boundary problem'.

Unlike some other techniques such as phase-field modelling which consider this interface as a diffused entity between the two phases [19], Stefan Problem defines the interface as a sharp entity. The mathematical equation applied in the domains of solid and liquid is a parabolic differential equation. A set of conditions, including Dirichlet and Stefan conditions are applicable to this interface. The Dirichlet condition sets the freezing temperature for solidification phenomenon and considers all associated factors like curvature

effect, surface effect and perturbation effects. The Stefan condition on the other hand predicts the rate of liquid to solid transformation. It states that the normal velocity of the interface separating the solid and the liquid phases (resulting in the evolution of latent heat during liquid-solid transformation) is proportional to the jump/rise of the temperature gradient across the interface [20]. The condition that defines the gradient in the liquid phase is called as Neumann condition. Our previous technical report [15] gives the detailed discussion on the physics and mathematical equations involved in the solidification process and various numerical approaches employed to solve these equations.

2.1.2. Radiative heat transfer and view factor

Radiation is a mode of heat transfer between two surfaces maintained at two different temperatures which does not require any medium for propagation as the heat transfer occurs in the form of waves. Total emissive power of a blackbody of area A and temperature T is given by the Stefan Boltzmann's law [21]:

$$q = A\sigma T^4 \quad \text{Eq.2.1}$$

Where σ is the Stefan-Boltzmann constant ($= 5.67 \times 10^{-8} \text{ W.m}^{-2}.\text{K}^{-4}$). The radiation emitted by a non-blackbody surface, often called a gray surface, is given by:

$$q = \varepsilon A\sigma T^4 \quad \text{Eq.2.2}$$

where ε is the emissivity of the surface. As radiation is proportional to the fourth power of temperature, it becomes more important at higher temperatures as compared to conduction.

While considering radiation exchanges between surfaces in a simulation problem, it is often assumed that the surfaces and elements taking part in radiation are separated by a non-participating media which does not affect such exchanges. The energy balance on the opaque surface is given by:

$$q = q_{emit} - q_{absorb} \quad \text{Eq.2.3}$$

For computing the total radiative energy balance in totality, a closed enclosure has to be considered [21]. This enclosure is assumed to be a simple isothermal surface having a constant average heat flux value across it [22]. Fig.2.1 shows such an enclosure in our case.

Apart from the radiative properties, radiation exchange between two surfaces is strongly dependent on surface geometries, their relative orientations and the distance between the surfaces; view factor takes care of these three factors. Considering two non-blackbody surfaces, A and B, A being the emitting and B the absorbing surface, at temperature T_a and T_b respectively, the energy radiated by surface A will be given by:

$$q_{a,emit} = q = \varepsilon_a A_a \sigma T_a^4 \quad \text{Eq.2.4}$$

The energy absorbed by surface B can be expressed by:

$$q_{b,absorbed} = F_{a \rightarrow b} \varepsilon_b A_b \sigma T_b^4 \quad \text{Eq.2.5},$$

where $F_{a \rightarrow b}$ is the view factor. Thus, the view factor can be defined as the ratio of the absorbed radiation to emitted radiation.

$$F_{a \rightarrow b} = \frac{q_{a,emitted}}{q_{b,absorbed}} \quad \text{Eq.2.6}$$

Fig.2.2. shows the schematic of view factor computation. Mathematically, it can be expressed as:

$$F_{a \rightarrow b} = \frac{1}{A_a} \int_{A_a} \int_{A_b} \frac{\cos\theta_a \cos\theta_b dA_a dA_b}{\pi R^2} \quad \text{Eq.2.7}$$

View factor follows the law of reciprocity (Eq.2.8) and the rule of summation, as (Eq.2.9)

$$A_a F_{a \rightarrow b} = A_b F_{b \rightarrow a} \quad \text{Eq.2.8}$$

$$\sum_{j=1}^N F_{ij} = 1 \quad \text{Eq.2.9}$$

In order to calculate the radiation exchange in an enclosure of N surfaces, a total of N^2 view factors should be calculated. Mathematically, the view factors on N surfaces are represented by a matrix:

$$\begin{bmatrix} F_{11} & \dots & F_{1N} \\ \vdots & \ddots & \vdots \\ F_{N1} & \dots & F_{NN} \end{bmatrix} \quad \text{Eq.2.10}$$

If the enclosure is divided into n surfaces that can't see each other and the total number of view factors, M, which must be calculated directly is given by:

$$M = \frac{N(N-1)}{2} - N \quad \text{Eq.2.11}$$

This number increases manifold when there are a number of radiating surfaces apart from the enclosure. In such a case, the computation of view factor requires huge computational resource.

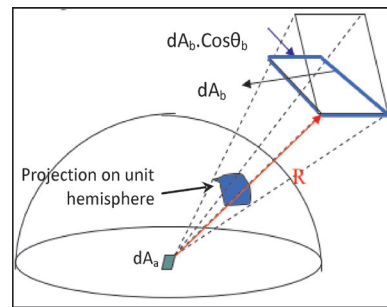


Fig.2.2 : View factor calculation [22].

2.2 Simulation

Simulations in this study were carried for cylindrical rod castings with different frequencies for updating of the view factor under varying process parameters. The process parameters that were considered are given in Table 2.1. Processing temperature is the temperature to which mould is heated and the investment casting is carried out. Pouring temperature is the temperature of the molten metal at the time of pouring. The mould withdrawal rate is the rate at which the mould is withdrawn from the heating chamber after pouring.

The pouring temperature, chill plate size and other furnace geometries were kept constant. The simulation

consists of five steps: (a) preparing the geometrical model and checking the model, (b) meshing, shell making and mesh repair, (c) applying boundary conditions (d) solution and (e) analysis of the results. Our earlier reports [20, 23] describe these steps in details. The features pertaining to the present study are given below.

Table 2.1. Values of process parameters used in simulation

Processing temperature(°C)	1450, 1525
Pouring temperature (°C)	1530
Mould withdrawal rate(mm.min ⁻¹)	3, 6, 9

2.2.1. Geometrical model preparation

ANSYS was used for geometrical modelling. Table 2.2 gives the general geometrical details of all the constituents considered in the model which includes the furnace, cylindrical rod casting, chill plate size, sprue, pouring cup and gate. In this study, seven rods were assumed to have been cast in a symmetrical distribution in a single shell, making the circular symmetry of the model as 7. Therefore, only one seventh of the whole geometry was modelled as shown in Fig.2.3. After the model was prepared, it was checked in **Geomesh environment** and then exported to **MeshCast** for meshing.

2.2.2. Meshing, shell making and mesh repair

To analyse the effect of mesh size on sensitivity of view factor update, two different sets of meshing were used; Table 2.3 shows their details. To capture the heat transfer

Table 2.2. Dimensions of the geometrical models involved in simulation (in mm)

Cast component diameter	12
Cast component height	210
Starter diameter	20
Starter height	20
Sprue rod height	290
Sprue rod diameter	18
Height of step between pouring cup and sprue rod	23
Diameter of step between pouring cup and sprue rod	20
Pouring cup height	67
Pouring cup top diameter	130
Pouring cup bottom diameter	60
Shell thickness	8
Shield thickness	5
Chill plate diameter	200
Chill plate height	50
Susceptor height	430
Furnace outer diameter	576
Susceptor inner diameter	480
Susceptor outer diameter	516
Furnace top thickness	50
Baffle thickness	13
Distance between baffle and chill plate	5

and mass transfer phenomena closely, the mesh intervals for casting component was kept the smallest. Since chill plate and furnace were bigger and no mass transfer was involved, their mesh sizes were kept bigger. The enclosure had the biggest mesh size as it was the biggest unit. Surface meshes generated using these sets are shown in Fig.2.4.

Table 2.3. Line mesh division for different volumes

Parts of the model	Maximum size of mesh (mm)	
	Set 1	Set 2
Rod	2	3
Gate	2	3
Sprue	3	4
Pouring cup	3	4
Chill plate	4	5
Furnace	8	10
Enclosure	20	30

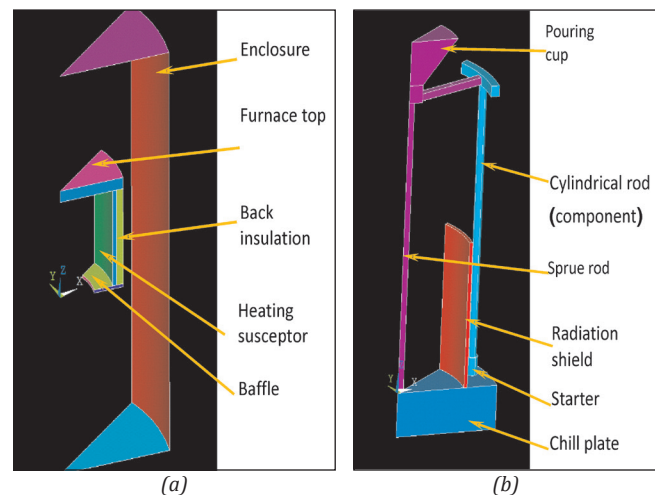


Fig.2.3 : Geometrical models of (a) cast and chill plate portion (b) furnace and enclosure

After the surface mesh was completed, a shell was built over the casting. The complete 8 mm thick shell was built in 2 layers, each 4 mm thick. After shell-making, the whole surface mesh was converted to volume mesh. During this operation, interior nodes were generated. Generation of a node is typically accompanied by the generation of associated elements. Thus the number of nodes and elements increases several times during this step. Table 2.4 gives the number of elements and nodes in surface mesh of different sets. The number of elements of the enclosure is given in Table 2.5.

Table 2.4. Number of elements and nodes in the various models

Sets	Surface Mesh		Volume Mesh	
	Elements	Nodes	Elements	Nodes
Set1	47,164	23,100	2,82,288	57,268
Set2	26,527	12,897	1,84,648	37,144

Table 2.5. Number of elements and nodes in the enclosure in various sets

Sets	Elements	Nodes
Set 1	5,764	3,008
Set 2	2,490	1,329

2.2.3. Applying boundary conditions

Once the mesh was ready, the symmetry, volume properties, boundary conditions, initial conditions, process parameters and run parameters were assigned to the meshed model. The pouring of molten metal starts at 1190 s and the rate is so maintained that the mould fills in 4-5 s. In other words, a pouring rate of 0.27 kg s⁻¹ has been considered. The mould is allowed to withdraw in 5 s after the pouring is complete. The mould withdrawal sequence in terms of position of the mould with time for three withdrawal rates (i.e. 3, 6 and 9 mm.min⁻¹) is shown in Table 2.6.

Out of all the boundary conditions, our focus was on the update frequency of the view factor. This factor comes under run parameters. The ProCAST software defines the update frequency in two ways: one is the time interval and the other is the distance interval. Defining the view factor update by time interval means that view factor is updated after a particular time interval, whereas defining it by distance interval means that view factor is updated after the mould has moved by a particular distance. As is shown in Table 2.6, the mould is stationary up to 1200 s after which it starts moving with a constant velocity till it comes out of the furnace completely. Therefore, the VFUI in this study is defined as the periodic distance after which the view factor is updated.

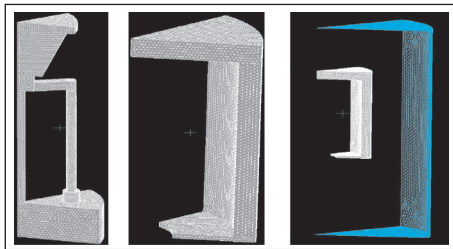


Fig.2.4 : Surface mesh of (a) cast and chill plate portion, (b) furnace portion and (c) the furnace with enclosure.

Table 2.6. The position of mould with respect to time at different withdrawal rates (WR)

Mould position	Time (s) for different withdrawal rates		
	3	6	9
0	0	0	0
0	1200	1200	1200
280	6800	4000	3067
280	7300	4500	3500

Thus, if the view factor update frequency is 5, the solid angles between every element taking part in radiation were recalculated and the view factor was updated

after every 5 mm withdrawal of the mould. The distance intervals used for update frequency in the present simulation were 1, 2, 5, 10 and 20 mm.

2.2.4. Solution

After incorporating all boundary conditions, twenty-five simulation runs were carried out on a single core work-station. The time taken (in hours) to complete a simulation run under various combinations of mould withdrawal rate and view factor update frequency (Table 2.7). The time taken for one set of view factor calculation, the number of view factor updates and time taken for calculation in different runs are shown in Table 2.8.

Table 2.7. Simulation time of different runs.

Set No	Mould withdrawal rate (mm.min ⁻¹)	Simulation run time at different VFUIs (VFUI) h,				
		1	2	5	10	20
1	3	80	46	24	16	14
	6	77	42.5	21	13.5	12
	9	73.5	40	18	11	10.5
2	3	31	20	13	10	9
	6	27.5	17	11	8.5	7
	9	25	14.5	9	7	5

Since the number of radiating elements under one set of meshing is constant, the time taken to calculate the view factor during each update is the same. Thus, the time taken for view factor calculation is independent of the mould withdrawal rate or processing temperature. However, the total simulation run time increases as the mould withdrawal rate decreases. Table 2.9 elaborates the reason behind this. The time needed for complete withdrawal of the mould and the number of time-steps needed for the solution (thermal and flow, view factor not included) have been given here.

As the mould withdrawal rate increases, the time required to withdraw the complete mould decreases and time-steps required to reach that time decrease. As the number of nodes is determined by mesh set, the time taken for a single time step is purely a function of mesh size. Thus the time required for thermal computations only, excluding the view factor computations, is number of steps (n_{th}) multiplied by the time taken for single step calculation ($t_{th,one}$).

$$t_{th} = n_{th} \times t_{th,one} \quad \text{Eq.2.12}$$

The number of time-steps depends on factors such as number of nodes and the element geometries. Another factor which contributes to the computation time is the time taken in flow computation during pouring. The time-step for flow calculations during pouring are very small as compared to thermal steps; hence the number of steps is large even for 5 seconds of pouring. The maximum time for each step was kept 0.01 s and for thermal calculations, it was 1 s.

Table 2.8. Simulation time of different runs
 (a) mesh set 1, (b) mesh set 2
 (a)

VFUI (mm)	Number of view factor calculations	Time taken for view factor calculation (h)	
		For one	For all
1	281	15	23.30
2	141		35.15
5	57		13.45
10	29		6.15
20	15		3.75

(b)

VFUI (mm)	Number of view factor calculations	Time taken for view factor calculation (h)	
		For one	For all
1	281	15	23.30
2	141		35.15
5	57		13.45
10	29		6.15
20	15		3.75

The total number of time-steps for the solution given in Table 2.8 is the number that includes steps for thermal calculations and flow calculations. The total run only has been given because it is very difficult to track record of the steps of thermal calculations and flow calculations separately during simulation. The time taken in flow calculation is dependent on the number of nodes present in cast component model, and not on the whole geometrical model. From Table 2.8 it is evident that the total number of time-steps also depends on the mould withdrawal rate; it decreases with increasing mould-withdrawal rate. Hence, the total run time decreases with faster mould withdrawal.

Thus, the total time taken in the simulation is given by the time taken in view factor calculations (t_{vf}) added to thermal calculation time ($t_{th} + t_{fl}$). This is the time which has been mentioned in the Table 2.6.

$$t = t_{th} + t_{vf} + t_{fl} \quad \text{Eq.2.13}$$

The first view factor is calculated as soon as the solution starts and successive calculations commence as the moulds come down. The total number of view factor updates (n_{vfu}) can be found by dividing the distance traversed by mould (D) by the distance interval for update (d).

$$n_{vfu} = \frac{D}{d} \quad \text{Eq.2.14}$$

Hence, the total number of view factor calculation is given by adding one to the number of view factor updates. Hence, we can write:

$$n_{vf} = n_{vfu} + 1 \quad \text{Eq.2.15}$$

The time taken in the view factor computation can be written as:

$$t_{vf} = n_{vf} \times t_{vf,one} \quad \text{Eq.2.16}$$

Table 2.9. Number of time steps in different runs.

Mould withdrawal rate(mm/min)	Process time (s)	No. of Time Steps (except view factor calculation)
3	7300	9800
6	4500	6240
9	3500	5030

The distance that the mould traverses in our simulation is 280 mm. From the Table 2.4, Table 2.5 and Table 2.8 it can be noted that for an increase of ~78% (from 26,527 in set 2 to 47,164 in set 1) in surface elements and of ~131% (from 2,490 in set 2 to 5,764 in set 1) in enclosure elements, the time taken to compute the view factor in one set increases three times. Thus it is evident from the Tables 2.7 and 2.8 that view factor calculation consumes a substantial proportion of time out of the whole run time.

From the above discussion it is evident that normally the simulation run time is independent of the processing temperature. However, the simulation run time changes if the number of nodes on which the temperature load is given is changed, even if the total number of nodes and elements in the geometry remains the same. This is true with every load, though this was not applicable in our case.

2.2.5. Analysis of the results

After the simulations were completed, thermal evolution, thermal profile, thermal gradient, cooling rate and solidification speeds were computed for different simulation runs and the effect of view factor update frequency was studied. The effect of processing parameters (viz. mould withdrawal rate and mesh size) on the sensitivity was also studied.

3. Results and Discussion

The results are discussed in two parts. The effect of view factor update on various parameters of solidification has been considered first. The effect of process parameters and mesh size on the sensitisation has been discussed subsequently.

3.1. Selection of point and profile

In author's previous report [24], it was discussed in detail about the selection of profile for analysing the results. The same scheme has been used here. The rod profile used is the profile located on the central axis of rod. This has been shown in in Fig. 3.1 (a). Three points have been chosen for discussion. The first point is just above the starter (i.e. at 15 mm from the chill plate), the second point is the midpoint of the rod (i.e. at 90 mm from the chill plate) and the third is at the top of the rod, just below the meeting point with the gate extending from the pouring cup (at 162 mm from chill plate). Fig.3.1 (b) shows the location of these three points. While analysing the results,

only casting component has been studied. The casting parts of sprue rod, gates and pouring cup have not been considered.

3.2. Effect of VFUI (VFUI)

A change in VFUI is expected to have a direct effect on heat exchanges with external ambience through radiation. This, in turn, would affect the temperature profiles and solidification parameters such as cooling rates, thermal gradients and solidification rates that is achieved in simulation. A frequent update of view factor is in complete agreement with the real radiation effect of the

heating or cooling atmosphere and other radiation heat exchanges; on the other hand, a delayed update with longer period fails to explain this effect.

In the following sections the effect of update interval on the factors mentioned above is going to be qualitatively analysed. Since a frequent view factor update also means a longer simulation time, the selection of an optimum view factor update frequency value has been made in such a way that the computation time is not extremely long as well as the accuracy of the computed values is not significantly compromised. All the results in this section pertain to mesh set 1 with a processing temperature of 1450 °C and mould withdrawal rate of 6 mm/min.

3.2.1. Effect on thermal evolution and thermal profile

In our discussion, the exit of any point say A has been treated in a particular manner. During its exit the point has to pass through the thickness of the exit baffle. When the point touches the start of the exit baffle, we will call it as the start of exit of the point or that the point has started to come out [~~this sentence can be further simplified /shortened; please rewrite~~]. When the point leaves the end of the exit baffle, we will mark it as the completion of exit and say that the point is fully out of the furnace. The times corresponding to the start and end of exit are called as the time of start of exit and time of end of exit, and the time taken in completing the exit is the time taken for the point to traverse the distance equal to the thickness of the exit baffle. In the present case, it is 13 mm (thickness of the baffle) divided by the 6 mm.min⁻¹ (withdrawal rate), which comes to 130 seconds.

It can be seen in the figure that till this time (i.e. 1200 – 1350 s) there is absolutely no effect of VFUI on thermal evolution and the curves corresponding to different intervals superimpose on one another. This is a clear indication that up to this height of casting, i.e. point A

remaining just inside the furnace, conduction through the chill plate is the dominant mechanism of heat dissipation. This is expected because of the fact that the point A is very close to the chill plate and the dominant mode of heat loss is conduction.

The temperature variation with time for point A using different update interval has been shown in the Fig.3.2a. The times corresponding to completion of pouring, starting of mould withdrawal and exit of point A have been marked in the plot. During the exit, Point A starts coming out of the furnace at $t = 1350$ s.

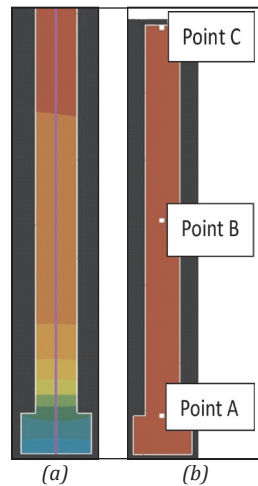
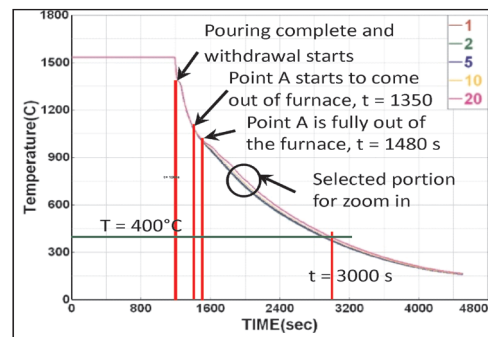
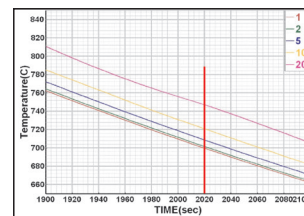


Fig.3.1 : (a) Selection of the profile, (b) The three points on rod



(a)



(b)

Fig.3.2 : Thermal evolution at the point A in the component (a) the full history and (b) close-up view of a selected portion.

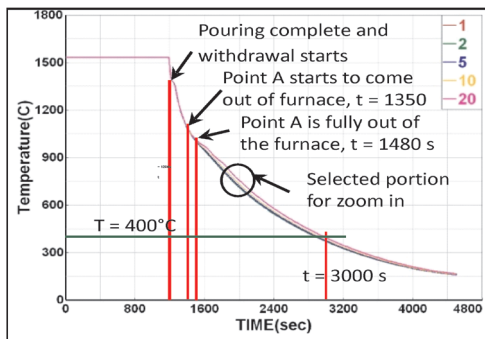
Although the effect of view factor update on heat extraction at point A becomes appreciable the moment point starts coming out of the furnace, the effect becomes appreciable only after it comes out completely. The effect becomes more apparent as the mould

keeps on coming out further; indicating the dominance of radiative heat transfer over conduction. This happens for about 3000 s and by that time the mould has been lowered by 180 mm (Fig.3.2 (a)). By this time point A has attained a low value of ~400 °C and the difference between this and the cooling atmosphere is not very large. Since the radiation effect is dominant at higher temperature differences (being a function of fourth power of the temperature as against conduction which is the function of the temperature) and due to the fact that this is the point which is very near to the chill plate where conduction is very strong, the radiation starts being dominated by the conduction heat transfer. Subsequently, the difference between the curves corresponding to different VFUIs starts becoming negligible.

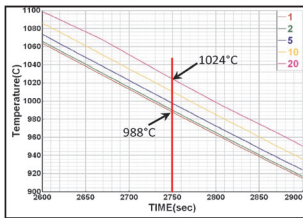
An enlarged view of the temperature profiles of the location encircled in Fig. 3.2 (a) is shown in Fig.3.2 (b). The figure shows that the temperature recorded is

higher as the update interval is increased. For example, at time $t = 2020$ s, the temperature of point A is 744°C , when a view factor update of 20 s is considered; this is significantly higher than the value (700°C) at VFUI of 1. This is due to the fact that at higher intervals of view factor, the computation is not able to fully capture the effect of heat dissipation.

Unlike point A, point B is much farther from the chill plate. As a result, the heat transfer at this point is not expected to be dominated by conduction and significant amount of radiative heat transfer can be expected. The effect on thermal evolution at the point B has been shown in Fig.3.3. The initial behaviour of this is same as the point A: the appreciable difference appears only after withdrawal by 15 mm and the temperature is $\sim 1425^\circ\text{C}$. The point is still inside furnace and starts coming out of the furnace at $t = 2100$ s and is fully out by 2230 s. By this time the difference between the various curves is well established (a closer picture is presented in Fig.3.3 (b)), showing that the primary mode of heat dissipation is radiation.



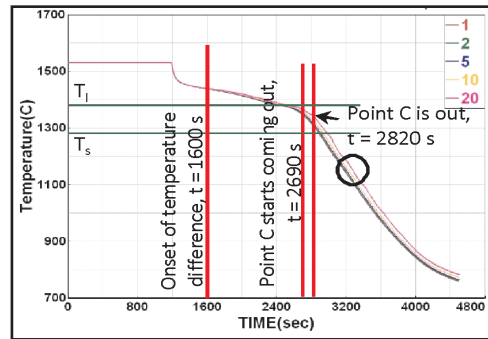
(a)



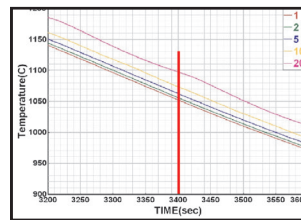
(b)

Fig.3.3 : Thermal evolution at the point B in the component (a) the full history and (b) close up view of a selected portion.

The difference in temperature at point B at 2750 s corresponding to view factor intervals of 1 and 20 is as large as 36°C , as evident from the enlarged view shown in Fig.3.3 (b). The effect of view factor interval on temperature variation at point C with time is also very similar to that observed at point B, as evident from Fig.3.4. The effect on thermal evolution at the point C has been shown in Fig.3.4. The point starts leaving the furnace at $t = 2690$ s and is fully out by 2820 s. Though the difference is present right from the point of time when point A and B started experiencing, but it becomes maximised only when the point comes out. This difference continues till the end, showing that the conduction has relatively a very weak role to play hereafter.



(a)



(b)

Fig.3.4 : Thermal evolution at the point C in the component (a) the full history and (b) close up view of a selected portion.

Table 3.1 shows the values of temperature difference at the three points for different VFUIs. The temperature at VFUI 1 was taken as the reference temperature while calculating the deviations. The deviation in temperatures for a given time in temperature-time plot obtained for all the view factor intervals with respect to the lowest view factor interval (VFI = 1) for all three points are provided in Table 3.1 (b). The corresponding temperatures at all three points are given in Table 3.1 (a).

Table 3.1. Temperature difference due to higher update intervals (a) the temperature values, and (b) the difference values.

(a)					
Point	Temperature measured using different update intervals				
	1	2	5	10	20
A ($t = 2000$ s)	710	712	719	731	754
B ($t = 2750$ s)	988	991	998	1012	1028
C ($t = 3400$ s)	1152	1155	1162	1174	1196

(b)					
Point	Temperature measured using different update intervals				
	1	2	5	10	20
A ($t = 2000$ s)	0	2	9	21	44
B ($t = 2750$ s)	0	3	10	22	40
C ($t = 3400$ s)	0	3	10	22	44

The time at which the temperature values have been taken are also marked in Figs.3.2 (b), 3.3 (b) and 3.4 (b). These times are a fair representative of the nature

of temperature versus time curves as these curves are almost parallel. The variation of temperature deviation with VFUI (VFUI) is plotted in Fig.3.5.

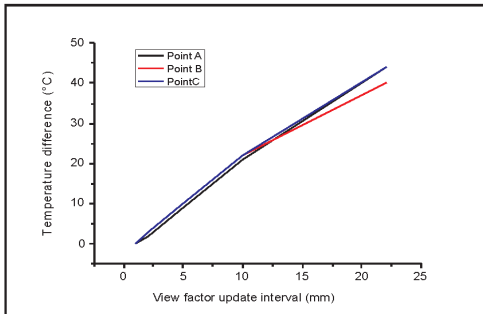


Fig.3.5 : Trend of temperature difference due to higher update intervals

It is observed in the figure that the deviation increases almost linearly with increase in VFUI. More interestingly, the temperature deviation value for any VFUI (with respect to VFUI = 1) is almost the same for all three points. For example, the deviation is 22 °C for VFUI = 10 for the points A, B and C (Table 3.1 (b)). This is to be expected considering the fact that the times at which deviation values have been taken corresponds to time when the points are completely outside the furnace and the temperature difference remains almost the same.

Fig.3.6 shows the central axis of the rod (the white line) for which profiles of different solidification parameters have been evaluated. This figure shows the location of the exit baffle marked by line z_2 . Here, the portion of the rod left to the line z_2 represents the portion that is out of the furnace, while the portion right to the line z_2 is inside the furnace. Variations of different solidification parameters along the rod axis can be plotted and these are called profiles. These profiles are the diagrams of solidification / thermal properties plotted against the distance traversed along the rod; this distance is measured as height from the chill plate which is at the bottom of the rod. These profiles depict the variation of temperature (or any other solidification / thermal property as the case may be) along the rod at a particular instant of time.

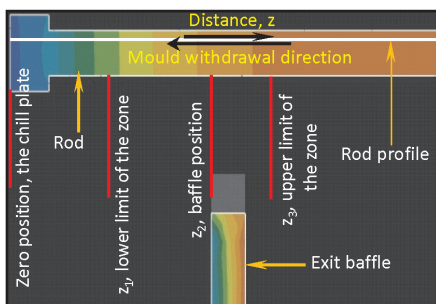
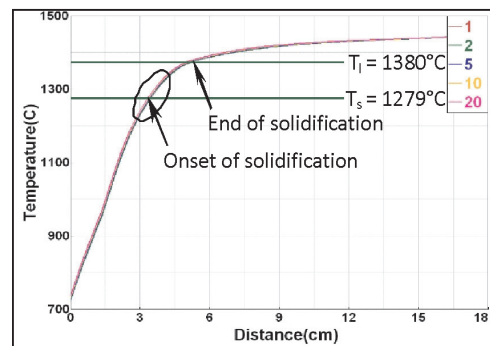


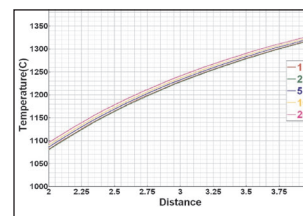
Fig.3.6 : Schematic of rod profile and baffle location.

Thermal profiles are shown in Fig.3.7 to Fig.3.10. These profiles belong to different times corresponding to different mould withdrawal heights. Fig.3.7 shows the

profile when mould is 20 mm out of the furnace, i.e. $z_2 = 20$ mm in Fig.3.6. Fig.3.7 (a) shows the thermal profiles in general and Fig.3.7 (b) shows the enlarged view for the encircled region of Fig.3.7 (a). It can be seen that the thermal profiles for different VFUI are very close to each other and a closer look suggests that the temperature difference between the profiles with VFUI of 1 mm and 20 mm is of the order of 15 °C. This is expected as at this point of time, the mould is largely inside the furnace and therefore, getting enough heat from the furnace. Further, conduction is the main heat dissipation mechanism at this early stage of directional solidification in investment casting process.



(a)



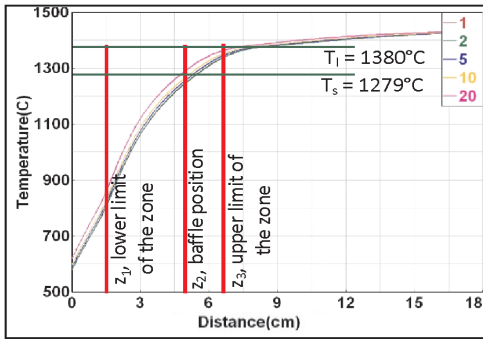
(b)

Fig. 3.7 : Temperature profile at different VFUI when mould is 20 mm out (a) for the whole rod, (b) for the encircled region of (a).

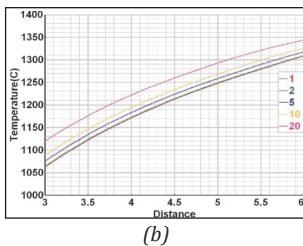
Fig.3.8 and Fig.3.9 show the thermal profiles corresponding to mould withdrawal height of 50 mm and 100 mm respectively. In these figures the thermal profiles corresponding to different VFUI-s are widely spaced as compared to the case when the mould was lowered by 20 mm (Fig.3.7). This suggests that the effect

of radiative heat loss begins to dominate with increasing withdrawal. There is another distinct feature in these figures: there is a zone, shown by the length bounded by lines z_1 and z_3 , where the difference between the profiles is the maximum. As we cross the line z_1 and move to the right, the difference between the profiles increases and after some distance it reaches a plateau. Upon crossing the line z_3 in right direction, the difference starts vanishing and is the minimum towards the end. Physically this means that there is a zone on the rod which covers the regions above and below the exit baffle location where the temperature difference is the maximum. This is the zone where heat dissipation due to radiation is most pronounced. The two lines z_1 and z_3 define the boundaries of this zone. This zone and the lines z_1 , z_2 and z_3 are also shown in the Fig.3.6.

As we move up the rod and cross the boundary z_3 , the heat dissipation due to radiation becomes negligible. As a result, the effect of VFUI becomes very low and temperature vs. distance plots in Fig.3.8 and 3.9 lie close to each other. In the same manner as we go down the rod and cross the line z_1 , the radiative dissipation weakens due to low temperature of the component, leading to lower differences with the radiating atmosphere.



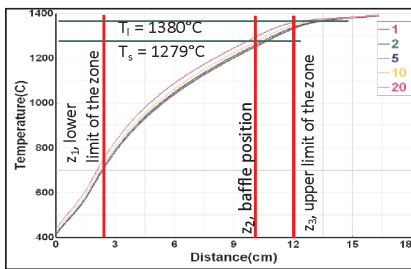
(a)



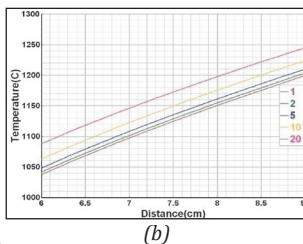
(b)

Fig.3.8. Temperature profile at different VFUI when mould is 50 mm out (a) for the whole rod (b) for the encircled region of (a).

A likely quantitative description of the radiative heat input from the furnace to the upper and middle ends of the rod and dissipative heat output from lower end to the atmosphere is provided below (assuming the following representative temperatures: furnace ~ 1450 °C, upper rod ~ 1400 °C, mid rod ~ 1300 °C, lower rod ~ 800 °C and atmosphere ~ 200 °C). The calculations that follow show that the radiative heat effect is almost three times stronger in the middle portions of the rod as compared to the upper and lower portions of the rod.



(a)



(b)

Fig.3.9 : Temperature profile at different VFUI when mould is 100 mm out (a) for the whole rod, (b) for the encircled region of (a).

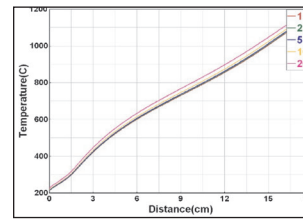
This is why the difference between the temperature lines increases in this segment of the rod.

$$Q_{f \rightarrow \text{rod, upper}} \propto 1723^4 - 1673^4 = 9.79 \times 10^{11}$$

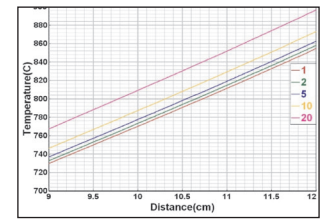
$$Q_{f \rightarrow \text{rod, mid}} \propto 1723^4 - 1573^4 = 26.91 \times 10^{11}$$

$$Q_{\text{rod, lower} \rightarrow \text{atm}} \propto 973^4 - 473^4 = 8.46 \times 10^{11}$$

At 200 mm withdrawal, the mould is completely out of the furnace. The thermal profile at this instant is shown in Fig.3.10. It is evident that the difference between the temperature curves corresponding to different VFUI continuously increases right from the bottom of the rod to the top end. This effect of VFUI on the thermal profile along the rod, when it is completely out, is expected considering the fact that the temperature of the rod increases across the length of the rod and, therefore, the effect of radiative heat loss from the rod to environment would also increase.



(a)



(b)

Fig.3.10 : Temperature profile at different VFUI when mould is 200 mm out (a) for the whole rod, (b) for the encircled region of (a).

Table 3.2. Temperature deviation due to higher update intervals

Mould withdrawal (mm)	Temperature deviation at different values of VFUI				
	1	2	5	10	20
20 (z = 30 mm)	0	1	5	9	14
50 (z = 45 mm)	0	1	10	20	48
100 (z = 75 mm)	0	4	9	25	47
200 (z = 105 mm)	0	4	8	18	40

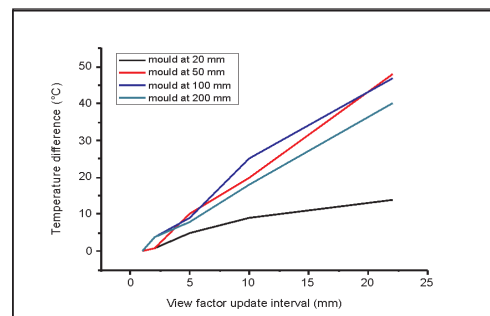


Fig.3.11 : Trend of temperature deviation at different mould withdrawal heights due to higher update intervals

The Fig.3.7 to 3.10 show that using a higher VFUI shifts the temperature-distance plots upwards. The maximum

upward shift, in terms of temperature difference, for the curves corresponding to VFUI of 2, 5, 10 and 20 mm with respect to the curve for VFUI = 1 are mentioned in Table 3.2. The distance points at which these values have been taken are indicated in the tables. These distance points fairly represent the nature of temperature deviations shown in Fig.3.11. The temperature difference shows a fairly linear variation with VFUI. It is clear from this figure that the temperature deviation caused by increasing VFUI rises, especially for the mould withdrawal values above 20 mm. This figure underlines the importance of choosing a low enough value VFUI for computation in order to minimise the error in temperature and other related parameters related to solidification.

3.2.2. Effect on mushy zone

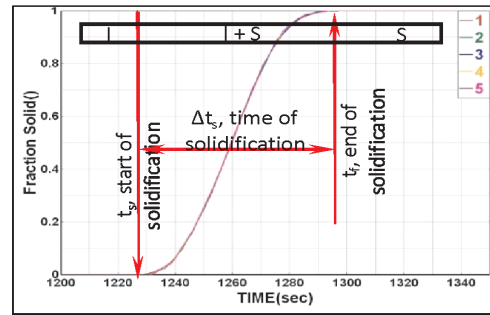
The study of mushy zone can reveal the effect of different thermal exchanges with further details. The variation in solid fraction with time for the three points A, B and C are shown in Fig.3.12. The graphs in these figures depict the variation of solid fraction with time. For complete liquid phase f_s is 0, for complete solid phase f_s is 1 and the region $0 < f_s < 1$ represents the mushy zone where both solid and liquid are present. The start of solidification (t_s), the end of solidification (t_f) and solidification time (Δt_s) are indicated in the Fig.3.12 (a). The liquid phase, the mushy zone and the solid phase are also shown here.

It is observed that the f_s versus time plots for point A under different update intervals superimpose each other. In all the cases, the solidification at point A starts at the same time, $t_s \sim 1227$ s, ends simultaneously at $t_f \sim 1295$ s and the solidification time is $\Delta t_s \sim 68$ s. In other words, the solidification at point A gets completed while the point is still inside the furnace (i.e. above the baffle).

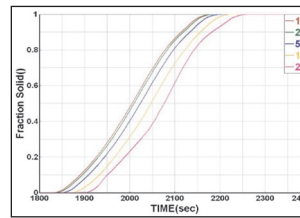
As the point comes out of the furnace only after 1480 s (see Fig.3.2 (a)), the effect of view factor at point A becomes apparent only beyond 1480 s, long after the solidification is complete. During solidification process (over which f_s changes with time), the dominant heat transfer mechanism at point A is conduction through the chill plate as this point is very close to it and radiative heat transfer is negligible. As a result, no effect of VFUI in terms of f_s vs time plot is observed for point A and all the curves superimpose over each other.

But, this is not the case with points B and C, which are away from the chill plate as compared to point A. Therefore, heat transfer at these two locations is dominated by radiation for a significant length of time.

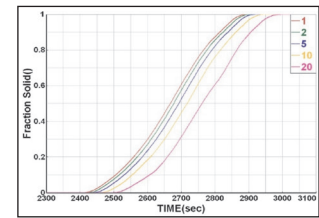
The solidification starts at $t_s \sim 1820$ s and $t_s \sim 2420$ s at points B and C respectively for VFUI = 1. From Fig.3.3 (a) and Fig.3.4 (a) it is noted that the onset of thermal difference is as early as 1600 s at these points. Hence, the start and end of solidification commence at different times at the points B and C under different VFUIs.



(a)



(b)



(c)

Fig.3.12 : Solid fraction profiles for (a) Point A, (b) Point B, and (c) Point C

The curves for higher update intervals lie at the right side relative to those of low update intervals; the solidification starts later where the capture of heat dissipation effect is lagging as shown in Fig.3.12 (b) and (c). This is in direct relation to the higher placement of temperature curves corresponding to higher update intervals in Fig.3.3 (a) and Fig.3.4 (a). Further, since in the solidification regime the slopes of different temperature curves are changing to some extent relative to each other, the solid fraction curves are not fully parallel to each other and hence the time taken for solidification is different at different update intervals.

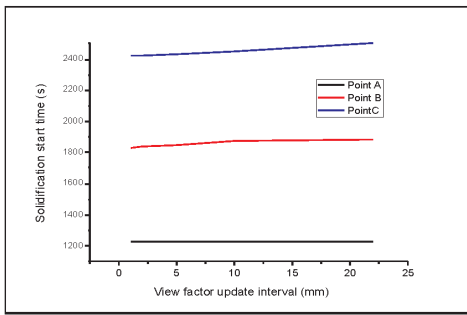
The onset of solidification as well as the solidification time are given in Table 3.3 and plotted in Fig.3.13. The plot shows that at higher update intervals the onset time of solidification and solidification times are longer, indicating a slightly longer mushy zone when radiation effects are not so frequently captured. The changes in solidification start time and solidification time of different points, as given in the Table 3.3, are also in complete agreement with the nature of data presented in the Table 3.1.

Solidification profiles at different mould withdrawals are shown in Fig.3.14. These profiles show the variation of fraction solid with the length of the rod indicating the solid, liquid and mushy portions of the rod. The onset of solidification is marked by the line p_1 and end is marked by the line p_s . Thus, the regions on rod which lie left to the line p_s is completely solid, the region which lies right to the line p_1 is completely liquid and the region bounded by the two lines represent the mushy zone where liquid and solid phases coexist. The three regions are shown in the Fig.3.14 (a).

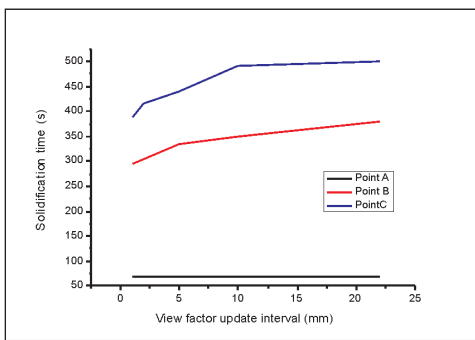
Table 3.3. Solidification at different point under different update intervals (a) onset, and (b) solidification time.

(a)					
Point	Onset of solidification at different VFUIs (s)				
	1	2	5	10	20
A	1227	1227	1227	1227	1227
B	1830	1840	1850	1875	1885
C	2420	2425	2430	2450	2500

(b)					
Point	Solidification time at different VFUIs (s)				
	1	2	5	10	20
A	68	68	68	68	68
B	295	305	335	350	380
C	390	415	440	490	500



(a)



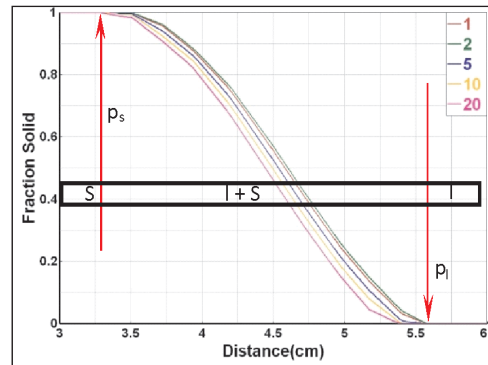
(b)

Fig.3.13 : (a) Onset of solidification and (b) Solidification time, at different points under various update intervals

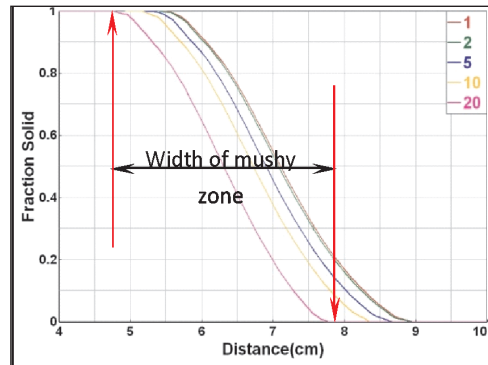
The length of mould withdrawals considered here are 20 mm, 50 mm and 100 mm; 200 mm is not considered here because by this time the complete rod is solid. It is observed from Fig.3.14 that at a particular instance (or at a particular length of mould withdrawal) the mushy zone is located lower on the rod at higher update intervals.

This result can also be derived from the temperature profiles shown in Fig.3.8, where it is observed that the thermal profiles corresponding to higher update intervals are located higher and left as compared to the profiles related to lower update intervals. It means that the liquidus and solidus lines intersect the profiles related

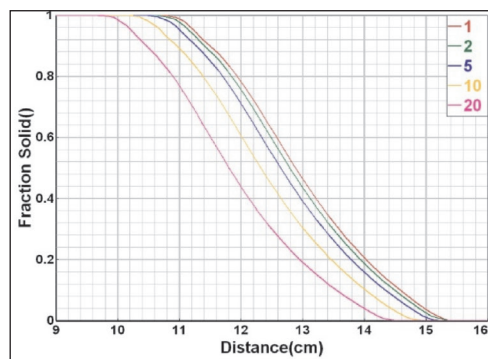
to higher update intervals prior to the intersection with profiles related to lower update intervals. As a result the mushy zone comes down the cast rod.



(a)



(b)



(c)

Fig.3.14 : Solidification profiles of rod when mould is (a) 20 mm down, (b) 50 mm down, and (c) 100 mm down

Table 3.4. Mushy zone features (a) position of mushy zone, and (b) mushy zone width.

(a)					
Mould withdrawal (mm)	Position of mushy zone w.r.t. baffle at different VFUI (mm)				
	1	2	5	10	20
20	4.3	4.1	4.0	3.7	3
50	-3.8	-4.0	-5.2	-7.4	-10.9
100	0	0	-1.8	-5.0	-9.6

Mould withdrawal (mm)	(b) Mushy zone width at different VFUI (mm)				
	1	2	5	10	20
20	4.3	4.1	4.0	3.7	3
50	-3.8	-4.0	-5.2	-7.4	-10.9
100	0	0	-1.8	-5.0	-9.6

Mushy zone location and its width at a particular mould withdrawal have been given in Table 3.4 and plotted in Fig.3.15. The positional variation of mushy zone on the rod with VFUI for any given withdrawal rate is consistent with the effect of VFUI on the temperature variation along the rod shown earlier in Fig.3.7 to 3.9. At higher VFUI, temperature vs. distance curve is pushed higher for any withdrawal rate, which means that the corresponding mushy zone moves closer to the chill plate, which is also reflected from Fig.3.14.

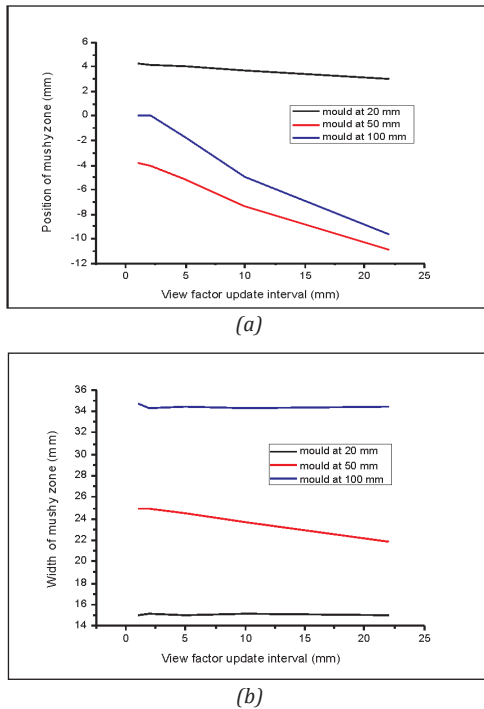


Fig.3.15 : Mushy zone features (a) position of mushy zone, and (b) mushy zone width.

3.2.3. Effect on solidification parameters

In this section the effect of VFUI on solidification parameters such as thermal gradient (G), cooling rate (L) and solidification front speed (R) is discussed. The calculation of these parameters, their general nature and significance have been discussed in author's previous publications [15, 23]. The change in behaviour of these properties under the application of different view factor update parameter will be elaborated here.

The solidification parameters have been computed at 1350 °C. In other words, as the temperature of any point

along the rod axis shown in Fig.3.6 reaches 1350 °C, the parameters are calculated. Fig.3.16 and Fig.3.17 show the variation in axial and radial thermal gradients along the central axis of the rod under different VFUIs.

The thermal gradients are linked to the thermal evolution; therefore the factors affecting the thermal profile of the rod would also be evident in the thermal gradients. It is observed in Fig.3.16 that the axial thermal gradient (G_z) curves for update intervals 1 mm, 2mm and 5 mm lie very much over each other and there is slight deviation in case of update-interval of 10. However, the curve corresponding to 20 mm update-interval shows significant deviation difference.

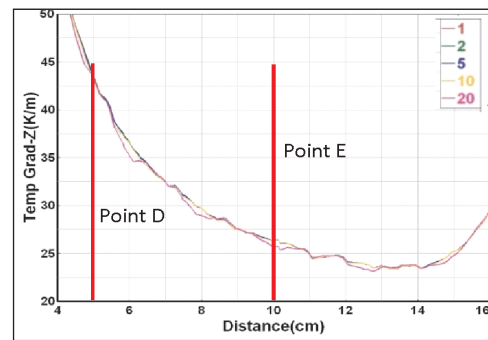


Fig.3.16 : Effect of update interval on axial thermal gradient.

The thermal gradient is calculated by computing the slope of tangents to the temperature profiles shown in Fig.3.7 to Fig.3.10 at a particular point, 1350 °C in our case. Fig.3.18 shows the thermal profiles of the two points D (at a height of 50 mm) and E (at a height of 100 mm) at update-interval of 1 and 20. These points are shown in Fig.3.16.

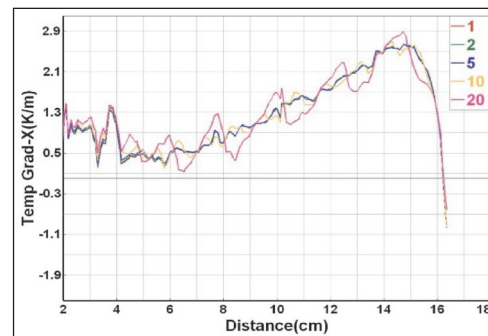


Fig.3.17 : Effect of update interval on radial thermal gradient.

The profiles belong to different point of time because the points D and E reach 1350 °C at different time instants. It is observed that while intersecting the abscissa for $T = 1350$ °C, the curves for 20 mm update interval are slightly flatter as compared to 1 mm curves. Hence, the gradient at 20 mm interval update is supposed to be lower. It indicates that at higher update intervals the accuracy in calculating thermal gradients is lost, the bigger the interval the bigger the inaccuracy. Fig.3.17 shows that the

accuracy of radial thermal gradient is lost considerably in case of 10 mm update-interval, and even grossly with 20 mm update-interval.

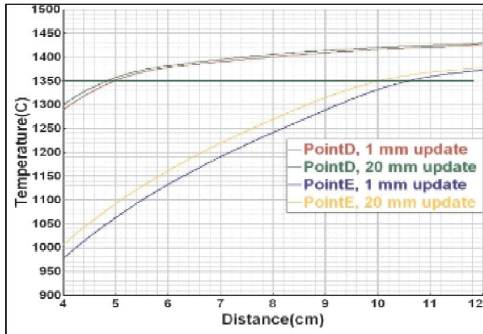


Fig.3.18 : Computation of thermal gradient from temperature profiles.

The effect of VFUI can also be seen in terms of cooling rate along the length of the rod. Cooling rate has been plotted as a function of distance from chill plate along rod length in Fig.3.19. The cooling rate is calculated by computing the slope of tangents to the temperature curves shown in Fig.3.2 to Fig.3.5 at 1350 °C. As expected, large VFUI-values such as 10 and 20 mm have a significant effect on the accuracy of the cooling rates as the curves corresponding to such high VFUI show large fluctuations, while the curves for 1, 2 and 5 are coherent. The initial portions of the cooling rate curve are very much similar as conduction is the main factor responsible for cooling in the initial portions.

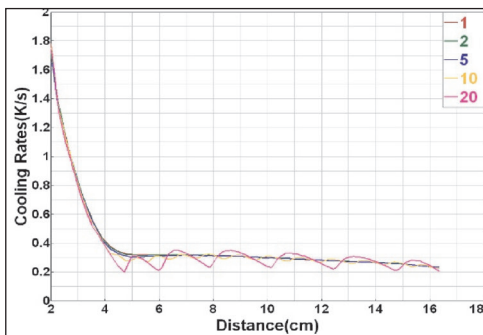


Fig.3.19 : Effect of update interval on cooling rate.

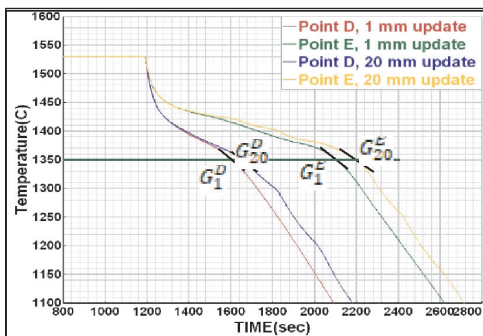


Fig.3.20 : Computation of thermal gradient from temperature diagrams.

Fig.3.20 shows the thermal curve of the two points shown in Fig.3.16. Tangents drawn to these curves at points D and E are shown in Fig.3.20 which show that cooling rate at point E is lower in case of 20 mm update interval as compared to that in case of 1 mm update interval.

The effect of VFUI on solidification rate has been shown in Fig.3.21. The solidification rate is expressed in terms of the isotherm velocity, which is the velocity of the isotherm at 1350 °C.

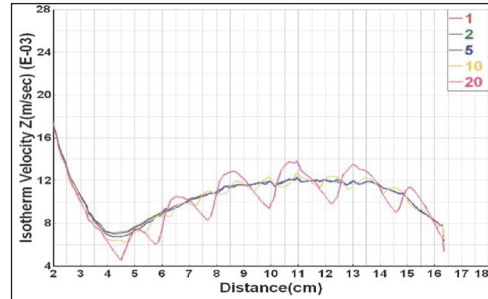


Fig.3.21 : Effect of update interval on solidification rate.

The effect on solidification rate is similar to the effect on cooling rate because of the fact that solidification rate is directly proportional to the cooling rate and the thermal gradient. The accuracy in capturing the solidification front speed is also hampered badly at higher update intervals such as 10 and 20 mm.

3.3. Effects of other factors on sensitisation caused by VFUI

In the previous section, a detailed analysis on the effect of VFUI on various solidification parameters in investment casting has been carried out. In this section, the effect of other factors on this sensitisation due to VFUI has been discussed. Three crucial factors will be discussed; they are the mesh size and process parameters like mould withdrawal rate and processing temperature. Since the solidification profiles and solidification parameters are related to temperature, thermal consideration is appropriate for a comparative study.

3.3.1. Mould withdrawal rate

Mould withdrawal rate is an important process parameter in investment casting of directional solidification process. Table 3.5 shows the temperature deviation for the three points A, B and C (Fig.3.1) for the simulations carried out at three different mould withdrawal rates: 3, 6 and 9 mm.min⁻¹. The temperature at VFUI = 1 is the base temperature here. These values have been plotted in Fig.3.22.

Table 3.5 and Fig.3.22 show that the sensitisation due to VFUI is weakly affected by change in the mould withdrawal rate. Though the lines for lower mould withdrawal effect are placed higher, the difference between the two lines is marginal. Further, this difference tends to disappear at points located higher on the rod.

Table 3.5. Effect of mould withdrawal rate on temperature deviation due to higher VFUI (a) point A, (b) point B, and (c) point C.

(a)					
Mould withdrawal (mm)	Temperature deviation at different update intervals (°C)				
	1	2	5	10	20
3	0	3	11	23	46
6	0	2	9	21	44
9	0	2	7	17	39

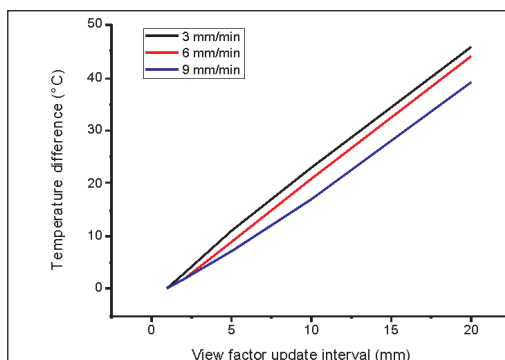
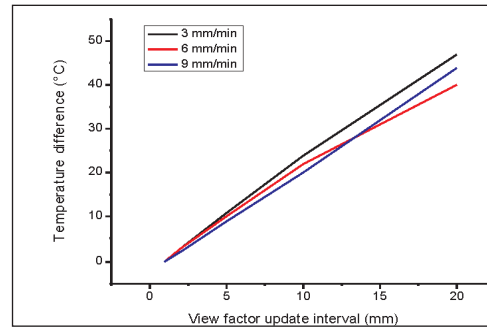
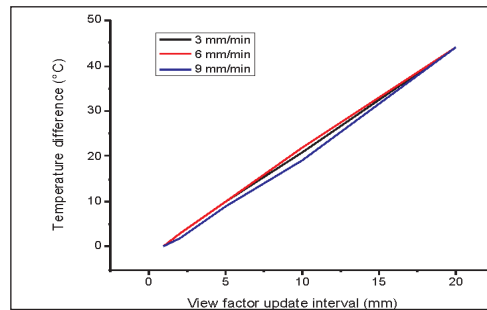
(b)					
Mould withdrawal (mm)	Temperature deviation at different update intervals (°C)				
	1	2	5	10	20
3	0	3	11	24	47
6	0	3	10	22	40
9	0	2	9	20	44

(c)					
Mould withdrawal (mm)	Temperature deviation at different update intervals (°C)				
	1	2	5	10	20
3	0	3	10	21	44
6	0	3	10	22	44
9	0	2	9	19	44

3.3.2. Processing temperature

Processing temperature is another important process parameter affecting the investment casting process. This factor determines the heat input to the component undergoing casting. Table 3.6 shows the temperature differences for the three points A, B and C for the simulations carried out at two different processing temperatures: 1450 °C and 1525 °C. These values are plotted in Fig.3.23.

As the above mentioned table and figure show, even the process temperature does not significantly alter the effect of sensitization irrespective of the locations (A, B or C) on the rod.


(a)

(b)

(c)
Fig.3.22 : Effect of mould withdrawal rate on sensitization due to view factor update. a) point A, (b) point B, and (c) point C.

3.3.3. Mesh size

Typically, a very coarse mesh would not closely capture the various transitions in a simulation. A very fine mesh on the other hand may be redundant and hugely increase the computation time. In the present case, the effect of mesh size on absolute temperature values and solidification parameters has not been considered. Instead, its relative effect on the influence of VFUI has been considered. Table 3.7 shows the temperature differences for the three points A, B and C for the simulations carried out at two different mesh sets: set 1 and set 2. These values have been plotted in Fig.3.24.

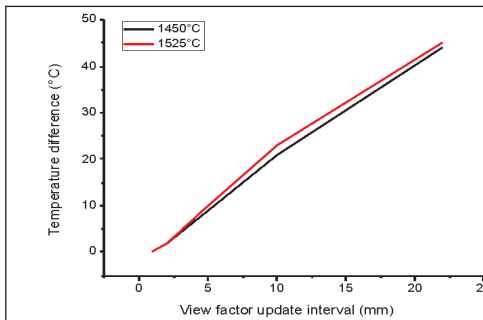
The Table 3.7 and Fig.3.24 indicate that the effect of mesh size on sensitization due to VFUI is much stronger in lower portions of the rod (point A). However, as we go up the rod (point B and C) this effect reduces. If the mesh is very coarse, the effect on this sensitization may be larger due to very poor capturing of the solidification phenomenon.

Table 3.6. Effect of processing temperature on temperature deviation due to VFUI (a) point A, (b) point B, and (c) point C.

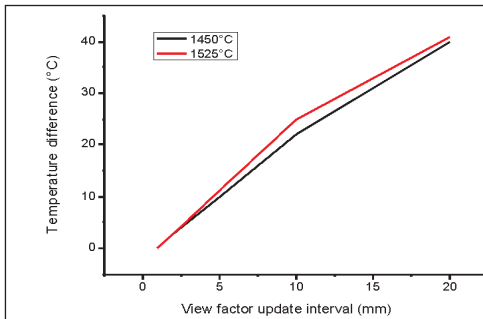
(a)					
Processing temperature (°C)	Temperature deviation at different update intervals (°C)				
	1	2	5	10	20
1450	0	2	9	21	44
1525	0	2	10	23	45

(b)					
Processing temperature (°C)	Temperature deviation at different update intervals (°C)				
	1	2	5	10	20
1450	0	3	10	22	40
1525	0	3	11	25	41

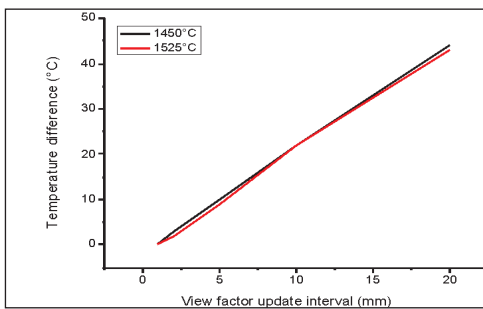
(c)					
Processing temperature (°C)	Temperature deviation at different update intervals (°C)				
	1	2	5	10	20
1450	0	3	10	22	44
1525	0	2	9	22	43



(a)



(b)



(c)

Fig.3.23 : Effect of processing temperature on sensitization due to view factor update. (a) point A, (b) point B, and (c) point C.

3.4. The optimum update interval

In previous sections, the effect of VFUI on various solidification parameters has been discussed. An update

interval needs to be chosen in simulation in such a way that it would lead to the least inaccuracy in the computational results. At the same time, the chosen interval should also not disproportionately increase the computational time. The solution run-times taken by different intervals have also been shown in Table 2.6 and are plotted here in Fig.3.25.

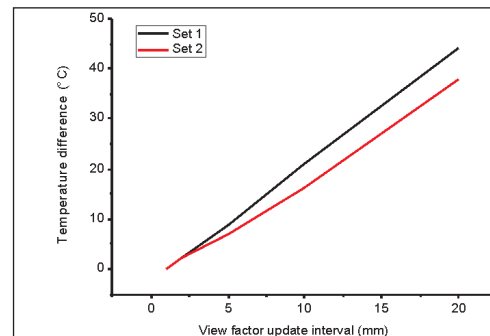
Table 3.7. Effect of mesh size on temperature deviation due to VFUI (a) point A, (b) point B, and (c) point C.

(a)					
Mesh size	Temperature deviation at different update intervals (°C)				
	1	2	5	10	20
1	0	2	9	21	44
2	0	2	7	16	38

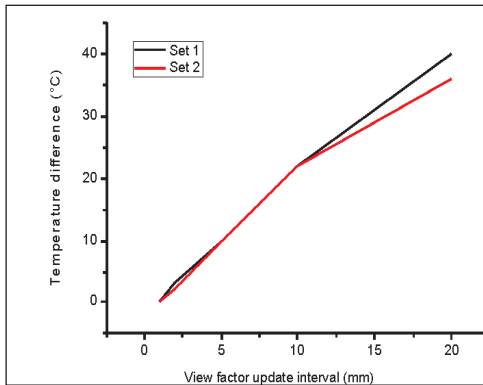
(b)					
Mesh size	Temperature deviation at different update intervals (°C)				
	1	2	5	10	20
1	0	3	10	22	40
2	0	2	10	22	36

(c)					
Mesh size	Temperature deviation at different update intervals (°C)				
	1	2	5	10	20
1	0	3	10	22	44
2	0	2	9	22	42

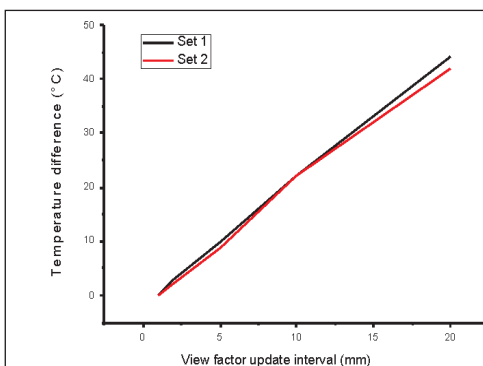
A superimposition of this curve with the temperature difference curve is presented in Fig.3.26. This figure suggests that the VFUI of 5 mm can be accepted as an optimum choice from the point of view of computation time and accuracy (encircled region). At this update interval the solution run time is not very large (~ 15-30 h) and the captured radiative heat exchanges are also acceptably accurate.



(a)



(b)



(c)

Fig.3.24 : Effect of mesh size on sensitization due to view factor update.(a) point A, (b) point B, and (c) point C.

Reducing the VFUI below 5 mm, say 1 mm, leads to a temperature accuracy improvement of only 8-10 °C and negligible improvement in the accuracies in thermal gradient, cooling rate and solidification rate; however, the computation time increases to 80 h from 25 h. Therefore, at a VFUI of 5 mm, a substantial computation time is saved without losing the accuracy in capturing the solidification effects. In this analysis, since the effects have been studied for different points located on different parts of the casting, the choice of 5 mm as the VFUI can be considered appropriate for all geometries.

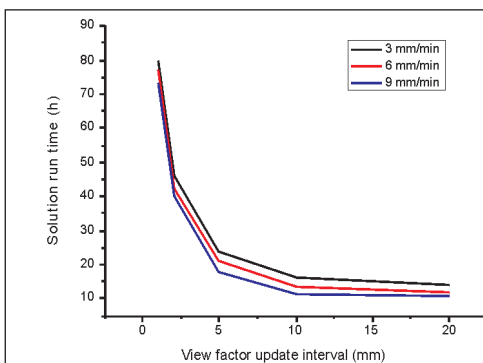


Fig.3.25 : Effect of view factor update on run time.

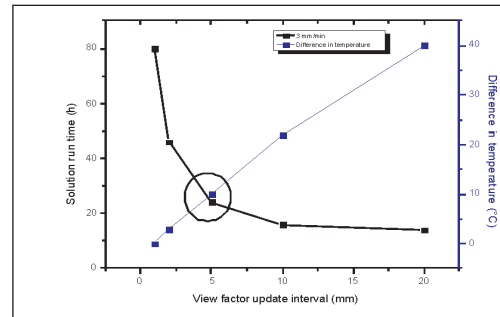


Fig.3.26 : Superimposition of temperature difference and run time.

4. Summary

The present simulation has examined the effect of VFUI in case of directionally solidified investment casting of superalloys. VFUI values of 1, 2, 5, 10 and 20 mm have been used for simulation. It is found that VFUI has a marked effect on the thermal profiles and solidification parameters. At values of high intervals such as 10 and 20 mm, the inaccuracy in capturing the results is large. At intervals as low as 1 and 2 mm, the process simulation time increases manifold. This limits the frequency to be used during simulation.

Such simulations at different processing parameters and mesh sizes reveal that the qualitative sensitisation due to VFUI at all parameters and the used mesh sets is retained with minimal quantitative change. However, use of a very coarse mesh may greatly affect these results because it fails to capture heat exchange especially due to conduction in the lower parts of the component and at initial solidification stage. Based on these simulation results, a view factor update parameter of 5 mm seems to be optimum as it saves considerable simulation time without causing significant loss in accuracies in the computation results.

Acknowledgements

The authors are thankful to DRDO and the Director, DMRL for permission to publish this technical report. The authors wish to thank all the staff and scientists of DSG for their cooperation and support. The authors thank the team of reviewers and editors of Metal News for many painstaking corrections which improved the presentability and readability of this special semi-S&T article.

References

1. J R Davis (Ed.), Directionally solidified and single crystal superalloys, Heat Resistant Materials – ASM Specialty Handbook, ASM International, Materials Park, OH, 1997, p. 255.
2. R C Reed, The Superalloys Fundamentals and Applications, 1st ed., Cambridge University Press, New York, 2006, p. 2.

3. M Donachie Jr. and S Donachie, Superalloys: a Technical Guide, 2nd ed. ASM International, Materials Park, OH, 2002, p. 20.
4. D Blavette, P Caron and T Khan in S Reichman et al., editors. Superalloys, Warrendale, USA; TMS, 1988, p. 305.
5. G L Erickson, JOM, TMS, Warrendale, PA, 1995 (4), p. 47.
6. M Konter and M Thuman, J. Mat. Proc. Technol., 2001 (117), p.386.
7. S H I Zhengxing, L Li Jianping and F U Hengzhi, Chinese Journal Metallurgical Science and Technol., 1990 (6), p. 167.
8. T M Pollock, Journal of Propulsion and Power, 2006, 22 (2), p.361.
9. J D Miller, Heat Extraction and Dendritic Growth During Directional Solidification of Single-Crystal Nickel-Base Superalloys, PhD Thesis, Department of Materials Science and Engineering, University of Michigan, 2011.
10. C Liu, J Shen, J Zhang and L Lou, Journal of Material Science and Technology, 2010, 26 (4), p. 304.
11. H. Leuenberger and R. A. Person, Compilation of Radiation Shape Factors for Cylindrical Assemblies, The American society of mechanical engineers, 1956, (59 A) p.144.
12. H. Fredriksson and U. Akerlind, Solidification and Crystallization Processing in Metals and Alloys, John Wiley & Sons Ltd., West Sussex, UK, 2012, p. 276.
13. B Canter and K O' Reilly, Solidification and Casting, IOP Publishing Ltd., Bristol, 2003, p. 106.
14. W. Kurtz and D. J. Fisher, Fundamentals of Solidification, Trans Tech Publications, USA, 1998, p. 6.
15. Kumar Saurabh, Satyapal Singh, N Hazari, D Chatterjee, Venkat and Niranjana Das, DMRL Technical Report, DRDO-DMRL-DSG-069-2014.
16. A Karma and W-J Rappel, Phys. Rev. E, 1998 (57), p. 4323.
17. G Segal, K Vuik, and F Vermoleny, Journal of Computational Physics, 1998 (141), p.1.
18. S Chen, B Merriman, S Osher, P Smereka, Journal of Computational Physics, 1997 (135), p. 8.
19. D Juric, G Tryggvason, Journal of Computational Physics, 1996 (123), p. 127.
20. J. Crank, Free and Moving Boundary Problems, Clarendon Press, Oxford, 1984.
21. T L Bergman and F P Incropera, Introduction to Heat Transfer, 6th Ed., John Wiley and Sons, New Jersey, 2011, p. 102.
22. J H Lienhard IV and J H Lienhard IV, A Heat Transfer Textbook, 3rd Ed., Philagiston Press, Cambridge, USA, 2006, p. 550.
23. Kumar Saurabh and Satyapal Singh, DMRL Technical Report, DRDO-DMRL-DSG-147-2016.

Advertisers' Index	
<i>Name of the Organisations</i>	<i>Page Nos.</i>
Hindalco Industries Ltd	2nd Cover
Chennai Metco Pvt Ltd	27
ARP/AR&DB, DMSRDE	28
Pragati Defence Systems Pvt Ltd	29
Durgapur Steel Plant	30
PTC Industries Limited	33
JSW Steel Ltd	34
Tata Steel Ltd	3rd Cover



World Class Products
Made in India - Exported worldwide

*Microstructure
Analysis for
QC and Research.*



Chennai Metco

www.chennaimetco.com



रक्षा अनुसंधान एवं विकास संगठन
रक्षा मंत्रालय, भारत सरकार
DEFENCE RESEARCH & DEVELOPMENT ORGANISATION
Ministry of Defence, Government of India

Aeronautics Research & Development Board

Vision

Make India technologically strong by establishing world class cutting edge aeronautical science and technology base to provide our Defence, Space and Civil Aviation sectors a decisive edge by equipping them with internationally competitive systems and solutions.

Mission

To encourage and fund basic and applied research in pertinent scientific disciplines directly relevant to our aeronautical systems needed for future by enabling and supporting emerging talents, particularly in academic and research institutions to create and evolve a potential knowledge-base system applicable to future aeronautics needs of the country.

Charter

- To formulate research, design and development programmes in aeronautics and allied sciences, keeping in view future needs of the country specifically with respect to aircraft, helicopter, missiles and all other airborne vehicles.
- To implement such programmes through appropriate institutions and individuals by sponsoring research, design and development projects, creating/ improving infrastructure facilities deemed necessary, while ensuring that they are suitably monitored.
- To promote in all possible ways such educational and training programmes as may be considered necessary for ensuring that adequate manpower of requisite quality becomes available to various aeronautical organizations in the country.
- To promote all relevant R&D activities in the country through appropriate scientific meetings, provisions of support for participation of Indian and foreign scientists in such meetings, conduct of relevant competitions as well as other training and visiting programmes within India and abroad as may fall within the scope of the programmes mentioned at sub para (a) above.
- Dissemination of appropriate technical information through journals and documents, encouragement of individual and collective efforts and nurturing of young talent by institutions with suitable awards, scholarships etc. Organization of necessary centralized services related documentation, software, data-link etc. and in all such other ways that the Board may determine from time to time.

Panels & Chairman

Aerodynamics Panel Dr S Pandian Prof. Vikram Sarabhai Distinguished Professor & Ex- Director & DS, SHAR	Propulsion Panel Dr V Ramanujachari National Centre for Combustion Research & Development (NCCRD), IIT Madras, Chennai
Aerospace Resources Panel Dr N Eswara Prasad OS & Ex-Director, DMSRDE (DRDO), Knp.-13	UNMANNED AERO SYSTEMS PANEL Shri PS Krishnan DS & Ex-Director, ADE, Bangalore-560075
Materials & Manufacturing Panel Dr DK Das, Scientist H Group Head (DSG), DMRL (DRDO) Hyd. - 58	Structures Panel Dr Makarand Joshi Scientist G, R&DE (E), DRDO, Pune-411015
GTMAP Prof. Amol A Gokhale, IITB, Chairman	Systems / Systems Engineering Panel Shri APVS Prasad Scientist H, CE, CEMILAC, DRDO, Bangalore



Single action
**QUICK RELEASE
OVERVEST** with quick reassembly

Very simple and intuitive quick release system - easy to don or doff the vest in split seconds

Activated safety mechanism to prevent accidental release of vest

40% lighter protection from handgun ammunition, RCC's and FSP's with improved energy absorption and dissipation levels

Optional stab protection

Front, back and side protection

Detachable neck, shoulder, groin protection



**COMFORTABLE &
ERGONOMIC DESIGN**

30% thinner, 50% more flexible

Ergonomic and extremely comfortable design

Rifle butt rests for added comfort

No metal parts for added security



All for a better quality of life

As a steel major, we are conscious of our role in India's fast forward industrial drive.

What we also consider with equal concern is the upliftment of the less fortunate people around us.

Under the banner of **Corporate Social Responsibility**, we put in our little big efforts for the community living around the plant, efforts that are designed to ensure a better quality of life for them.

Health care, education, occupation and industrial training including those for the handicapped, self-reliance through indirect employment, development of village infrastructure, recreation facilities are some of the areas we are concentrating on...A soul satisfying experience that we are committed to enhancing as we move along.



स्टील अथॉरिटी ऑफ इण्डिया लिमिटेड
STEEL AUTHORITY OF INDIA LIMITED

Durgapur Steel Plant
Durgapur – 713 203, West Bengal, India

News Updates National

RINL achieves record turnover in FY 2021-22, says CMD

Rashtriya Ispat Nigam Limited (RINL), the corporate entity of Visakhapatnam Steel Plant, has achieved a record turnover of Rs 28,215 crore in the 2021-22 financial year.

Presiding over the 40th annual general meeting of RINL in Visakhapatnam CMD Atul Bhatt said the company achieved earnings before interest, taxes, depreciation and amortisation (EBITDA) of Rs 3,469 crore, marking a growth of 148 per cent over the previous year.

"After six financial years, we have earned a positive Profit Before Tax with a cash profit of Rs 1,923 crore in 2021-22, thanks to the highest ever turnover," Bhatt said. The CMD said RINL registered best-ever performance in all important techno-economic parameters.

The Economic Times

DRDO conducts successful test flight of VSHORADS missile

The DRDO successfully flight tested the Very Short Range Air Defence System (VSHORADS) missile in Chandipur off the coast of Odisha. The VSHORADS is an air defence system designed and developed indigenously by Hyderabad-based Research Centre Imarat of the Defence Research and Development Organisation (DRDO).

"The DRDO conducted two successful test flight of the Very Short Range Air Defence System (VSHORADS)

missile on September 27 from a ground based portable launcher at the integrated test range, Chandipur, off the coast of Odisha," the defence ministry said in a statement.

"VSHORADS missile incorporates many novel technologies including miniaturized Reaction Control System (RCS) and integrated avionics, which have been successfully proven during the tests," the ministry said.

Defence Minister Rajnath Singh complimented and appreciated the efforts of DRDO and industry partners and said this new missile equipped with modern technologies will give further technological boost to the armed forces.

The Economic Times

Tata Steel gets land allotment letter to set up Rs 2,600 crore plant in Ludhiana

Punjab Chief Minister Bhagwant Mann handed over the land allotment letter to the Tata group for setting up its maiden scrap-based steel plant at an investment of Rs 2,600 crore in Ludhiana. The move is aimed at giving further fillip to industrial development in the state.

"We are committed for making Punjab a front runner in industrial sector and this maiden investment by Tata group in state is a step forward in this direction," IANS quoted Mann as saying during meeting with delegation led by Global CEO & Managing Director, Tata Steel Ltd, T.V. Narendran.

The Economic Times

Chapter Activities Bhubaneswar, Sunabeda, Rourkela, Kanpur, Pune

Bhubaneswar Chapter

IIM Bhubaneswar Chapter organised the Brahm Prakash Memorial Materials Quiz on 7th August, 2022 at SS Bhatnagar Hall, CSIR-IMMT, Bhubaneswar. The winning team was DAV Public School, Pokhripur, Bhubaneswar and the runner-up team was from BJEM school, BJB Nagar, Bhubaneswar. Over 60 attendees had witnessed the Quiz competition.



Left to right : Shri. H.K. Tripathy, Chairman, IIM Bhubaneswar chapter, Prof. S. Basu, Director, CSIR-IMMT with Winners team: Mr. Soumya Subhrakanta and Priyanshu Pritam Nayak, Std: XII, DAV Public School, Pokhripur, Bhubaneswar

Sunabeda Chapter

The Annual Metals and Materials quiz competition was organised by IIM Sunabeda Chapter on 10th August 2022. Six teams (each team comprising of two students) from different educational institutions nearby Sunabeda have participated in the quiz competition. Out of them two best



Felicitations to the Winners

teams were selected so as to represent the chapter and participate in the upcoming BPMMQ-2022 competition

organised by The IIM Kalpakkam Chapter. Winners were awarded by Shri Kallol Bhattacharyya, Vice- Chairman, IIM Sunabeda Chapter.

Rourkela Chapter

IIM Rourkela Chapter organised the Science Quiz-2022 with special focus on the role of Materials Sciences and Metallurgy in human civilisation, ancient archaeology, industrial engineering and technology developments at Rourkela Club on 28th August, 2022. Students of class XI and XII forming 20 groups from different schools of Rourkela participated in the Quiz.

Sri Shivam Singh and Sri Ayushman Dash from Dr. ANK DAV School were adjudged the winning team and Sri Yashovardhana Kiran and Sri Aman Singh from Delhi Public School was declared the runners-up team. These two teams were nominated for participating in the final event (BPMMQ 2022) held at Kalpakkam. Mr. S R Suryawanshi, ED (Works) and Chairman, IIM Rourkela Chapter was the Chief Guest of the programme and he handed over the trophies and mementoes to the winners.



Kanpur Chapter

Prof. N. K. Batra Metals & Materials Quiz - 2022

The annual Prof. N. K. Batra Metals & Materials Quiz-2022 was jointly organised by the Dept. of Materials Science and Engineering, IIT Kanpur and IIM Kanpur Chapter on September 3, 2022 at IIT Kanpur. The quiz witnessed enthusiastic participation from 27 teams representing 14 different schools in Kanpur. This annual event is for the students of Class XI and XII, and is aimed at inculcating their interests in Materials and Metallurgical Engineering.

The event started with the welcoming address of Prof. Kallol Mondal, Head, Dep of Materials Science and Engineering, IIT Kanpur. In his address, he highlighted the contributions of late Prof. N. K. Batra, and this quiz is named after him. Prof. Amarendra Kumar Singh, Chairman IIM Kanpur Chapter, also extended a warm welcome to all the participants and described about IIM and the quiz. Prof. Abhay Karandikar, Director, IIT Kanpur talked about the importance of materials and inaugurated the quiz. The successful conduction of the inaugural program was done by Prof. Sudhanshu Shekhar Singh, Secretary of IIM Kanpur Chapter.

As a part of the event, Prof. Manoj K. Harbola (Professor, Department of Physics, IIT Kanpur) delivered a talk

on “Entertainment with materials around us”, where he showed various experiments on materials used in day-to-day life. An exhibition was also organised by the students of MSE department wherein several models, such as organic light-emitting diodes, simulation-based experiments, crystal structure models, etc., were demonstrated to the students and teachers.

Mr. Anuz and Mr. Om Upadhyaya from Kendriya Vidyalaya, IIT Kanpur bagged the first position in the Prof. N. K. Batra Metals & Materials Quiz 2022. Mr. Harsh Jha and Mr. Abhay Chandra of Delhi Public School, Azaad Nagar, Kanpur were the runners-up.



Pune Chapter

IIM Pune Chapter organised Prof. Brahm Prakash Memorial Materials Quiz 2022 on 3rd Sept 2022. A total of 100 teams from 33 colleges & institutes registered for the quiz. Prof. S. P. Butee, HoD, Dept. of Metallurgy and Materials Science, addressed the participating students & teachers and briefed about Metallurgy & Material Science Engineering. Mr. Lalit Pahwa, Chairman, IIM Pune chapter, welcomed the participants and briefed on Prof. Brahm Prakash Memorial quiz and different activities carried out by Pune chapter. Dr. Bhanu Pant from Kalyani Centre for Technology and Innovation (KCTI), Pune, was the chief guest of this event. He enlightened the students on metals in Aerospace and interdisciplinary approach in today's era. The talk was very much appreciated by the students.

The winning team was Yogesh Kshirsagar & Tushar Banne from Fergusson college and the runners-up team was Pratik More and Krushna Mote from Dhage's chemistry classes. The winning teams were awarded certificates by Dr. Pahwa and Prof. Butee.

The program concluded with a vote of thanks by IIM student body general secretary Aditya Kuge from Dept. of Metallurgy and Materials Science, COEP.



PTC INDUSTRIES LIMITED

Manufacturer of

- 1) Titanium Castings**
- 2) Nickel Super Alloys Castings**
- 3) Hot Isostatic Pressurised Parts**
- 4) 5 Axis CNC Machining**

Components of Aero Engines, Rocket, Missiles, Submarines and Land based Defence equipments.



Advanced Manufacturing and Technology Centre

NH-25A, Sarai Sahjadi, Lucknow – 227101

E-mail – marketing1@ptcil.com ; Ph no. 0522-7111017 ; Fax no. 011-66173715



We make
the best,
even better.

JSW - A conglomerate worth \$13 Billion believes in transformation to make a better world every day

It takes a strong will to be ranked among India's top business houses. But it was stronger dreams and ambition that made us venture into the core sectors of Steel, Energy, Cement and Infrastructure. Our strength, state-of-the art technology and excellence in execution have helped us grow and that has helped India grow multi-fold. By harbouring dreams of transformation, focusing on sustainability and a philosophy; to give back to the country, the JSW Group is making a better world every day.

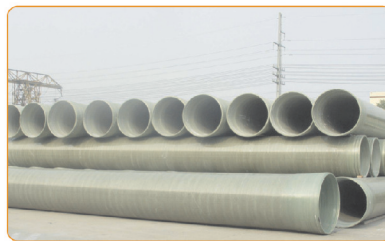
FUTURE-READY SOLUTIONS IN COMPOSITES

FOR NEW-GENERATION INDUSTRIES

Tata Steel is constantly exploring new frontiers of advanced materials to move towards an innovative and sustainable future. Our range of future-ready solutions crafted with composites are best suited to meet the evolving needs of core industries.



Tanks



Pipes



Pressure Vessels



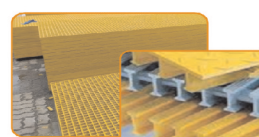
Mine Sleepers



Fencing & Movable Barricades



Conveyor Guards



Gratings



Railway Windows

NEW MATERIALS BUSINESS

An Initiative of Tata Steel

email: nmb.composite@tatasteel.com



International Conference
on
Corrosion and Coatings
(i3C)

Conference website: www.i3c.info

December 07-08, 2022

Jamshedpur, India

Organized by
IIM Jamshedpur Chapter
in association with
Tata Steel, CSIR-NML & NIT-Jamshedpur

